# LETTER

Oxytocin–dependent reopening of a social reward learning critical period with MDMA

Romain Nardou[1,2,3], Eastman M. Lewis[1,2,3], Rebecca Rothhaas[1,2,3], Ran Xu[4,5], Aimei Yang[4,5,6], Edward Boyden[4,5,6] & Gül Dölen[1,2,3]*

A critical period is a developmental epoch during which the nervous system is expressly sensitive to specific environmental stimuli that are required for proper circuit organization and learning. Mechanistic characterization of critical periods has revealed an important role for exuberant brain plasticity during early development, and for constraints that are imposed on these mechanisms as the brain matures[1]. In disease states, closure of critical periods limits the ability of the brain to adapt even when optimal conditions are restored. Thus, identification of manipulations that reopen critical periods has been a priority for translational neuroscience[2]. Here we provide evidence that developmental regulation of oxytocin-mediated synaptic plasticity (long-term depression) in the nucleus accumbens establishes a critical period for social reward learning. Furthermore, we show that a single dose of (+/−)-3,4-methylendioxymethamphetamine (MDMA) reopens the critical period for social reward learning and leads to a metaplastic upregulation of oxytocin-dependent long-term depression. MDMA-induced reopening of this critical period requires activation of oxytocin receptors in the nucleus accumbens, and is recapitulated by stimulation of oxytocin terminals in the nucleus accumbens. These findings have important implications for understanding the pathogenesis of neurodevelopmental diseases that are characterized by social impairments and of disorders that respond to social influence or are the result of social injury[3].

In juvenile mice, oxytocin (OT) evokes a unique form of synaptic plasticity, long-term depression (LTD), in the nucleus accumbens (NAc), and this cellular mechanism is correlated with social reward learning in vivo[4]. In this study, we began by examining the maturational profile of social conditioned place preference (social CPP; Fig. 1a) to determine whether this behaviour is constrained by a critical period in mice. Ages were chosen to span milestones in brain development, including weaning (postnatal day 21, P21), onset of puberty (P28), sexual maturity (P42), early adulthood (P60), and
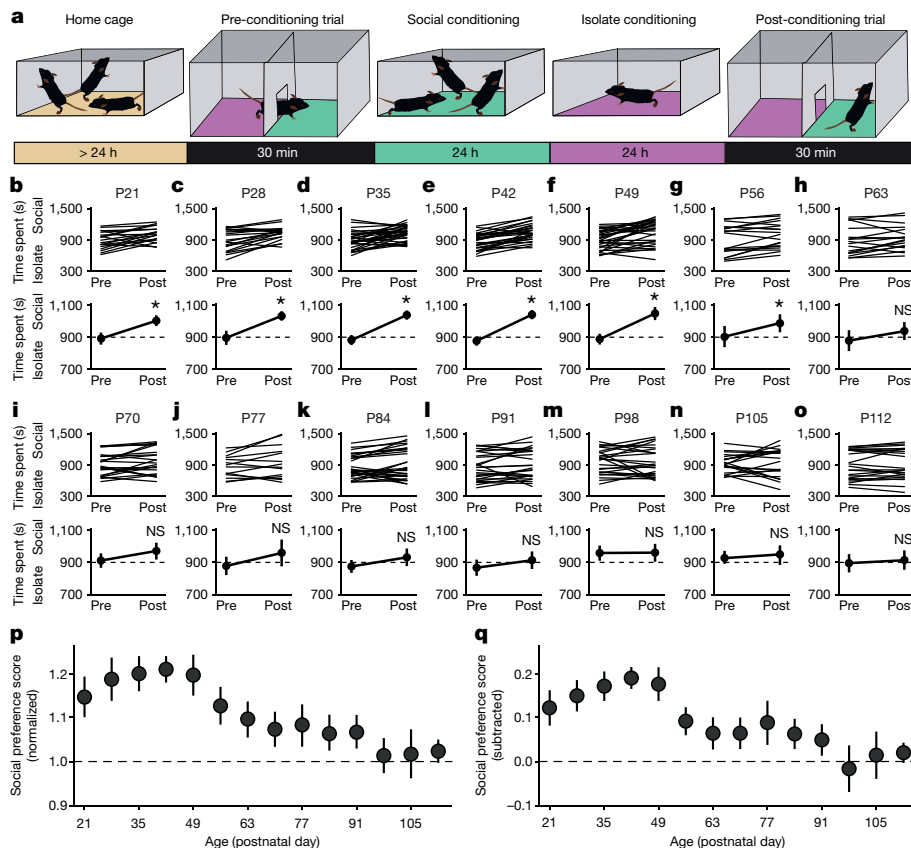
Fig. 1 | Social reward learning is constrained by a developmental critical period.
a, Protocol (top) and time course (bottom) illustrating social CPP assay. **b–o**, Individual (top) and average (bottom) responses of male mice from P21 to P112 reveal a significant developmental decline in the magnitude of social CPP (repeated measures ANOVA, $F_{(13,311)} = 3.119$, $P = 0.000217$). See Extended Data Table 1 for sample size and additional statistical comparisons. **p, q**, Comparison across ages using the normalized and subtracted social preference scores show that social CPP peaks at P42 and then declines until the closure of the critical period at P98 (normalized: one-way ANOVA, $F_{(13,311)} = 3.187$, $P = 0.000162$; subtracted: one-way ANOVA, $F_{(13,311)} = 3.060$, $P = 0.000279$). Data are presented as mean ± s.e.m. *$P < 0.05$; NS, comparisons not significant ($P > 0.05$).

[1]The Solomon H. Snyder Department of Neuroscience, Brain Science Institute, Johns Hopkins University School of Medicine, Baltimore, MD, USA. [2]The Solomon H. Snyder Department of Neuroscience, Wendy Klag Institute, Johns Hopkins University School of Medicine, Baltimore, MD, USA. [3]The Solomon H. Snyder Department of Neuroscience, Kavli Neuroscience Discovery Institute, Johns Hopkins University School of Medicine, Baltimore, MD, USA. [4]Department of Brain and Cognitive Sciences, MIT, Cambridge, MA, USA. [5]McGovern Institute, MIT, Cambridge, MA, USA. [6]Department of Biological Engineering, Media Laboratory, Koch Institute, MIT, Cambridge, MA, USA. *e-mail: gul@jhu.edu
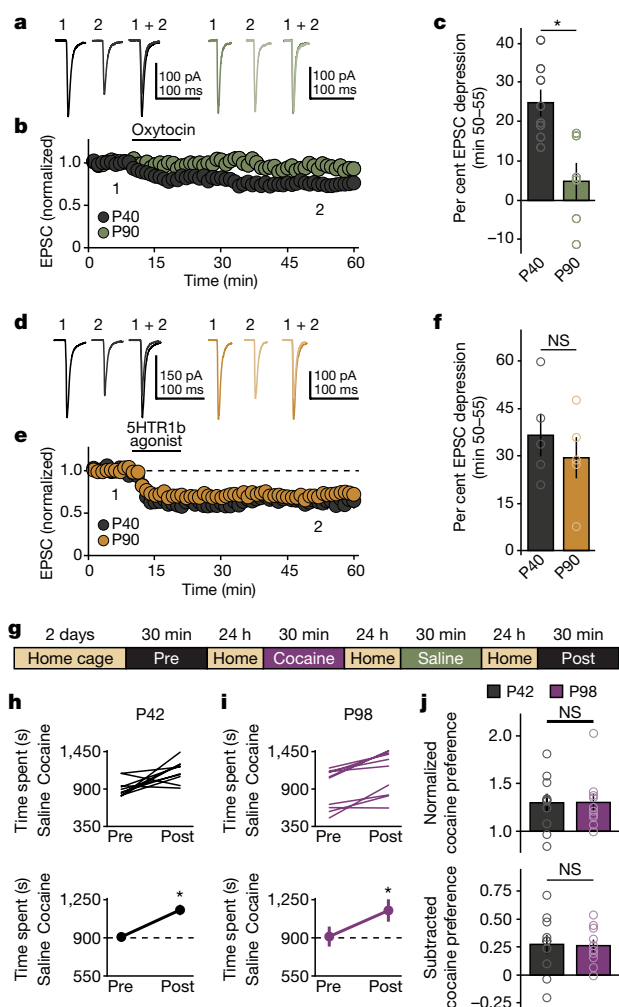
Fig. 2 | OT-induced LTD in the NAc is developmentally downregulated. a–c, OT-LTD. Representative traces (**a**) and summary time course (**b**) of EPSC amplitude over time in NAc MSNs from mice at P40 (black circles) versus P90 (green circles) following 10-min bath application of OT. **c**, OT-LTD is significantly decreased at P90 ($n = 6$ cells) compared to P40 ($n = 8$ cells; $t_{(12)} = -3.57$, $P = 0.004$). **d–f**, 5HTR1b-LTD. Representative traces (**d**), summary time course (**e**) and average post-treatment magnitude comparisons (**f**) reveal that EPSC depression in cells treated with a 5HTR1b agonist (CP-93129 dihydrochloride) does not differ between P40 (black circles, $n = 10$ cells) and P90 (orange circles, $n = 10$ cells) ($t_{(8)} = -0.765$, $P = 0.466$). **g–j**, Cocaine CPP. **g**, Experimental time course. **h, i**, Individual (top) and average (bottom) responses indicate increased preference for the cocaine-paired context (P42, $n = 10$ mice, $t_{(9)} = -3.244$, $P = 0.010$; P98, $n = 10$, $t_{(9)} = -4.962$, $P = 0.001$). **j**, Comparisons between P42 and P98 reveal no difference in normalized (top, $t_{(18)} = 0.003$, $P = 0.998$) and subtracted (bottom, $t_{(18)} = 0.138$, $P = 0.892$) cocaine preference. Data are presented as mean ± s.e.m. *$P < 0.05$; NS, comparisons not significant ($P > 0.05$). Two-tailed unpaired t-test for **c**, **f**, **j**; two-tailed paired t-test for **h**, **i**.

mature adulthood (P90) (Fig. 1b–o). We compared age groups using normalized and subtracted social preference scores (Fig. 1p, q); these data show that, in male mice, the magnitude of social CPP peaks at P42 and declines thereafter until the close of the critical period at P98 (Extended Data Table 1). This maturational profile is largely recapitulated in females (Extended Data Fig. 1). Notably, locomotor behaviours are similar between adolescent and adult mice (Extended Data Fig. 2), so it is unlikely that the effects of maturation on social CPP are due to a general decline in activity across development. These studies provide a comprehensive profile of social reward learning across maturation, and identify a critical period that constrains this behaviour.

To determine whether developmental changes in social reward learning behaviour correspond to a change in the expression of OT-dependent LTD (OT-LTD)[4], we recorded excitatory postsynaptic currents (EPSCs) from medium spiny neurons (MSNs) in acute NAc slices prepared from male mice at P40 and P90. The magnitude of LTD induced by bath application of OT (1 μM, 10 min) was significantly decreased at P90 compared to P40 (Fig. 2a–c). Retrograde labelling studies revealed no evidence for a maturational decline in the number of oxytocinergic inputs to the NAc (Extended Data Fig. 3). We also examined the magnitude of serotonin 1b receptor-mediated LTD (5HTR1b-LTD)[4]; bath application of the selective 5HTR1b agonist CP-93129 (2 μM, 10 min) induced robust LTD of EPSCs, the magnitude of which did not differ between ages (Fig. 2d–f). Finally, we also examined cocaine-induced (20, 10 or 5 mg kg^{-1}) CPP at P42 and P98, but found no difference in the magnitude of cocaine reward learning between ages (Fig. 2g–j, Extended Data Fig. 4). Together, these data provide evidence that selective regulation of OT-mediated synaptic plasticity in the NAc is at least one mechanism that underlies the establishment of a critical period for social reward learning.

We next investigated whether OT signalling mechanisms could be strategically targeted to reopen the critical period for social reward learning. OT does not cross the blood–brain barrier[5,6]; consistent with this observation, intraperitoneal injection of OT did not reinstate social reward learning in adult mice (Extended Data Fig. 5). Notably, the phenethylamine MDMA has been shown to stimulate OT neurons[7–9], raising the possibility that the prosocial effects of MDMA[10] might be the consequence of OT activity. To characterize the synaptic effects of MDMA in the NAc, we recorded EPSCs from MSNs in acute slices prepared from adolescent male mice. Bath application of MDMA (2 μM, 10 min) induced significant LTD, which was blocked by pre-incubation with an OT receptor antagonist (OTR-A, L-368,899, 5 μM; Fig. 3a–c), and occluded by OT-LTD (Extended Data Fig. 6a–c), indicating that these forms of synaptic plasticity share overlapping mechanisms. Consistent with a dominant role for MDMA binding at the serotonin transporter (SERT)[11–13] (but see ref. [14]), a SERT antagonist (fluoxetine, 10 μM) completely blocked MDMA-induced LTD (Extended Data Fig. 6d–f) but had no effect on the magnitude of OT-LTD (Extended Data Fig. 6d–f). Stimulation of OT release by MDMA and 5-HT in the hypothalamus requires 5HT1A and 5HT4 receptors[8,15,16]. In the NAc, MDMA-induced LTD was blocked by the 5HTR4 antagonist SB203186 (10 μM; Extended Data Fig. 6g–i), but not by the 5HTR1A antagonist WAY-100635 (10 nM and 10 μM; data not shown); again, these manipulations had no effect on the magnitude of OT-LTD (Extended Data Fig. 6g–i). Thus, MDMA induces synaptic plasticity in the NAc, and this plasticity requires activation of SERT, 5HTR4, and OTR.

We next investigated the potential of MDMA to reopen the critical period for social reward learning. We administered a single intraperitoneal dose of MDMA (10 mg kg^{-1}; determined empirically, Extended Data Fig. 7a–e) to adult mice (P96) and assessed the magnitude of social CPP 48 h later. Pretreatment with MDMA, but not saline, induced the reinstatement of social CPP measured at P98 (Fig. 3d–h). Further characterization of the effects of MDMA revealed that pretreatment with MDMA in a socially isolated setting failed to reinstate social reward learning in adulthood (Extended Data Fig. 7f–j). Examination of the time course of these effects revealed that reinstatement of social CPP began within 6 h of MDMA administration, lasted at least 2 weeks, and returned to the levels seen in saline-pretreated mice by 4 weeks (Extended Data Fig. 7k–r). Cocaine pretreatment (20 mg kg^{-1}) did not reinstate social reward learning in adult mice (Fig. 3i–m), and MDMA pretreatment had no effect on the magnitude of cocaine (20 mg kg^{-1}) CPP in adult mice (Extended Data Fig. 7s–v). Finally, we pretreated adult mice with MDMA and prepared acute slices containing the NAc 48 h later. The magnitude of OT-LTD was increased in slices prepared from MDMA-pretreated mice, compared with saline-pretreated control mice (Fig. 3n–p). These data provide evidence that MDMA pretreatment leads to the reopening of the critical period for social reward learning by inducing a metaplastic[17] reinstatement of OT-LTD in the NAc.
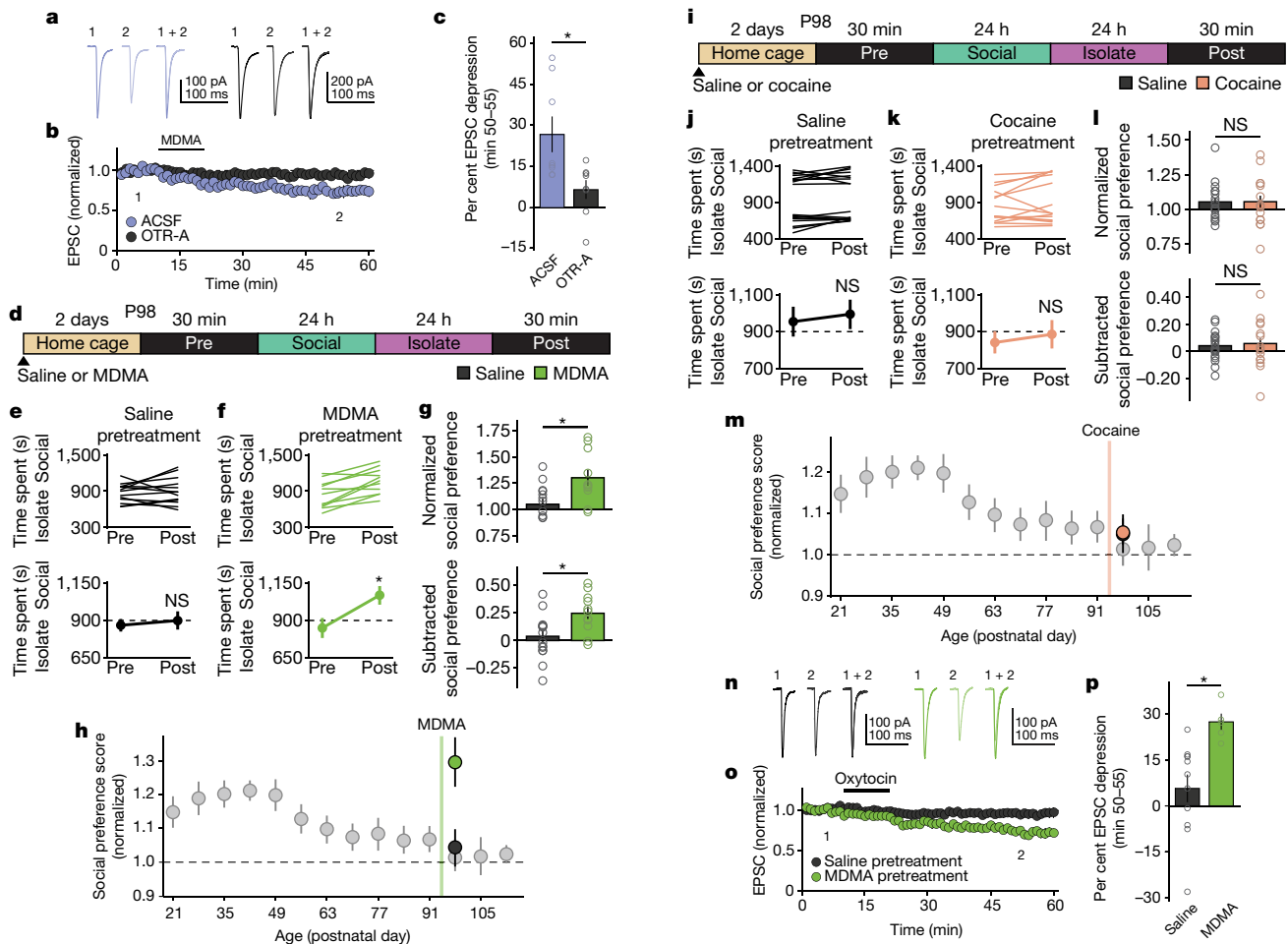
Fig. 3 | MDMA reinstates social reward learning and OT-LTD in adult mice. a–c, MDMA-LTD. Representative traces (**a**), summary time course (**b**), and average post-treatment magnitude comparisons (**c**) of EPSC amplitude reveal that OTR-A application (5 μM, black circles) prevents the induction of LTD by MDMA (2 μM, 10 min, blue circles) in NAc MSNs from juvenile mice ($n = 8$ cells, $t_{(14)} = -2.758$, $P = 0.015$). **d–m**, MDMA reopens critical period. Experimental time course of intraperitoneal (i.p.) drug pretreatment in social CPP (**d, i**). Individual (top) and average (bottom) responses of P98 mice indicate that mice pretreated with MDMA, but not saline or cocaine, develop a preference for the social bedding cue (**e, f**, saline ($n = 13$ mice, $t_{(12)} = -0.632$, $P = 0.539$), MDMA ($n = 11$ mice, $t_{(10)} = -4.563$, $P = 0.001$); **j, k**, saline ($n = 18$ mice, $t_{(17)} = -1.602$, $P = 0.127$), cocaine ($n = 15$ mice, $t_{(14)} = -1.067$, $P = 0.304$)). **g, l**, Comparisons reveal a significant increase in normalized (top, $t_{(22)} = -2.81$, $P = 0.01$) and subtracted (bottom, $t_{(22)} = -2.615$,

$P = 0.016$) social preference in MDMA- versus saline-pretreated mice (**g**), but no difference in normalized ($t_{(31)} = 0.07$, $P = 0.995$) and subtracted ($t_{(31)} = -0.176$, $P = 0.862$) social preference for cocaine versus saline (**l**). **h, m**, Normalized social preference in mice pretreated with MDMA versus saline (**h**) or cocaine versus saline (**m**) plotted against the developmental time course of untreated mice (replotted from Fig. 1q). **n–p**, MDMA induces metaplasticity. Representative traces (**n**), summary time course (**o**), and average post-treatment magnitude comparisons (**p**) of EPSC amplitude in MSNs at P90 reveal that OT-LTD magnitude is significantly increased in mice pretreated with MDMA ($n = 5$ cells, green circles) versus saline ($n = 11$ cells, black circles) ($t_{(14)} = -3.024$, $P = 0.009$). Data are presented as mean ± s.e.m. *$P < 0.05$; NS, comparisons not significant ($P > 0.05$). Two-tailed unpaired t-test for **c, g, l, p**; two-tailed paired t-test for **e, f, k, j**.

Next, we next sought to strengthen the causal link between the effects of MDMA and OT signalling mechanisms. Co-administration of MDMA with an OTR-A that can cross the blood–brain barrier (L-368,899, 7.5 mg kg⁻¹) prevented the reinstatement of social CPP in adulthood induced by MDMA pretreatment (Extended Data Fig. 8a–e). Pretreatment with the OTR-A alone did not alter the magnitude of social CPP in adult mice (Extended Data Fig. 8f–j). These effects can be localized to the NAc, as MDMA (11 μM) delivered directly to this brain region via bilateral cannulas 48 h before social CPP testing reinstated social reward learning in adults, and this effect was blocked by co-delivery of OTR-A (500 ng) to the NAc (Fig. 4a–e). Next, to determine whether OT is sufficient to reopen the critical period for social reward learning, we generated and validated an OT-2A-Flp optimized knock-in (OT-2A-Flp KI) mouse (Fig. 4f, Extended Data Fig. 9a–d, i). We also generated an AAV-CAG-₍Fon₎Chronos-TdTomato virus (Fig. 4g, Extended Data Fig. 9e–h, j) to molecularly target OT neurons for expression of Chronos, a channelrhodopsin protein with

enhanced stimulation kinetics[18]. In acute slices of the paraventricular nucleus (PVN) prepared from OT-2A-Flp KI mice previously injected with AAV-CAG-₍Fon₎Chronos-TdTomato, optical stimulation across a range of frequencies (10–40 Hz) reliably evoked action potentials in molecularly specified OT neurons (Fig. 4h). Consistent with our previous finding that OT-LTD is presynaptically expressed[4], pretreatment of acute slices from the NAc with optical stimulation (30 min, 5-ms pulse, 20 Hz, 15 mW) significantly decreased the frequency, but not the amplitude, of miniature EPSCs (mEPSCs) in MSNs treated with saline compared to those treated with OTR-A (Fig. 4i–m). Finally, mice received a single 30-min session of NAc OT terminal stimulation (5-ms pulse, 20 Hz, 20 mW) and were tested for social CPP 48 h later, at P98. Pretreatment with optogenetic stimulation of OT terminals in the NAc led to the expression of robust social CPP in OT-2A-Flp KI mice but not in C57BL/6 wild-type mice (Fig. 4n–r), indicating that this manipulation reopens the critical period for social reward learning. Together, these data provide direct evidence that MDMA-induced
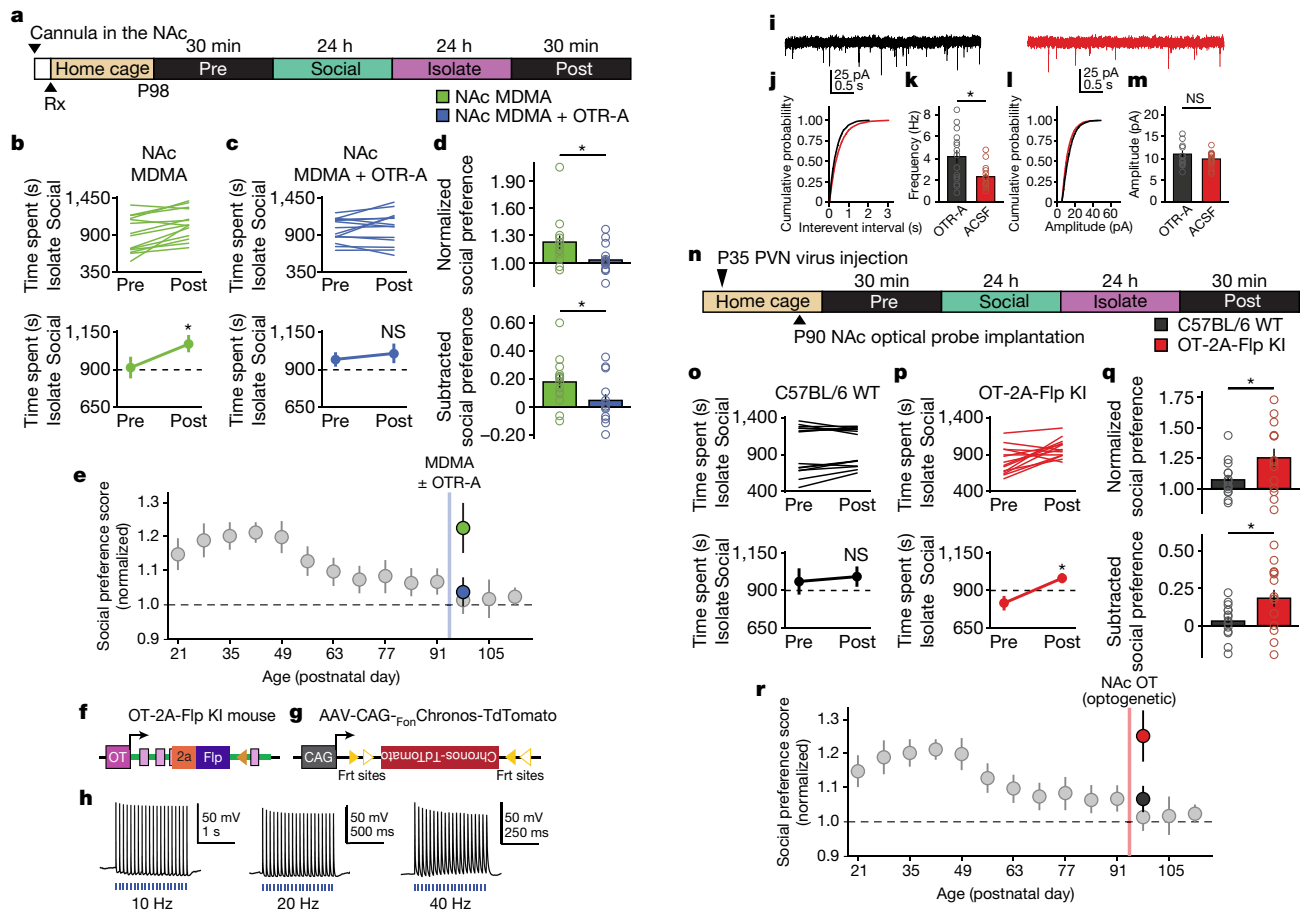
Fig. 4 | OT in the NAc is necessary and sufficient to reopen the critical period for social reward learning. a–e, OTR-A blocks MDMA-induced reopening of the critical period **a,** Experimental time course. **b, c,** Individual (top) and average (bottom) responses of mice following pretreatment with MDMA (**b,** $n = 14$ mice, $t_{(13)} = 3.86$, $P = 0.002$) or MDMA + OTR-A (**c,** $n = 14$ mice, $t_{(13)} = -1.061$, $P = 0.308$). **d,** Normalized (top, $t_{(26)} = 2.194$, $P = 0.037$) and subtracted (bottom, $t_{(26)} = 2.101$, $P = 0.045$) social preference scores are significantly decreased following delivery of MDMA + OTR-A versus MDMA alone to the NAc 48 h before social CPP. **e,** Normalized social preference in mice pretreated with MDMA or MDMA + OTR-A plotted against the developmental time course of untreated male mice (replotted from Fig. 1q). **f–q,** Optogenetics. Gene targeting in the OT-2A-Flp KI mouse (**f**) and the Flp-dependent Chronos-TdTomato (AAV-CAG-$_{Fon}$Chronos-TdTomato) construct (**g**). **h,** Current-clamp recordings of molecularly specified OT neurons in the PVN prepared from OT-2A-Flp KI mice injected with AAV-CAG-$_{Fon}$Chronos-TdTomato. Optical stimulation across a range of frequencies (10–40 Hz) reliably evoked action potentials. **i,** Representative mEPSCs recorded after 30 min optogenetic stimulation (5-ms pulse, 20 Hz, 15 mW) of OT terminals in NAc in the absence (left, black) or presence of OTR-A (5 μM, right, red). Cumulative probability (**j, l**) and average (**k, m**) comparisons reveal that mEPSC frequency (**j, k,** saline, $n = 16$ cells, OTR-A, $n = 15$, $t_{(29)} = 2.869$, $P = 0.008$) but not amplitude (**l, m,** $t_{(29)} = 1.425$, $P = 0.165$) is decreased in cells pretreated with OTR-A as compared to saline. **n,** Experimental time course. **o, p,** OT-2A-Flp KI mice ($n = 14$ mice, $t_{(13)} = -3.195$, $P = 0.007$) but not C57BL6/J wild-type mice ($n = 14$, $t_{(13)} = -1.286$, $P = 0.221$) exhibit robust social CPP after pretreatment with optical stimulation. **q,** Normalized (top, $t_{(26)} = -2.166$, $P = 0.040$) and subtracted (bottom, $t_{(26)} = -2.332$, $P = 0.028$) social preference scores are increased in OT-2A-Flp KI mice compared with C57BL6/J wild-type mice. **r,** Normalized social preference in OT-2A-Flp KI and C57BL6/J wild-type mice plotted against the developmental time course of untreated male mice (replotted from Fig. 1q). Data are presented as mean ± s.e.m. *$P < 0.05$; NS, comparisons not significant ($P > 0.05$). Two-tailed paired t-test for **b, c, o, p**; two-tailed unpaired t-test for **d, k, m, q**.

reopening of the critical period for social reward learning requires OTRs in the NAc and is recapitulated by stimulation of OT terminals in the NAc.

Cognitive neuroscientists have speculated on the existence of a critical period for social behaviour[19–23]. To our knowledge, these studies are the first to identify and characterize such a critical period by demonstrating that: (1) mice are maximally sensitive to social reward learning cues during adolescence (Fig. 1); (2) this sensitivity declines in adulthood (Fig. 1); and (3) these adaptations correspond to a maturational downregulation of OT-mediated synaptic plasticity in the NAc (Fig. 2a–c). Moreover, the results of our retrograde labelling studies (Extended Data Fig. 3) are consistent with previous reports that OT receptors[24], rather than oxytocinergic inputs, are downregulated during development. As 5HTR1b-LTD (Fig. 2d–f) is not developmentally downregulated, it is unlikely that a maturational decline in glutamatergic signalling mechanisms could account for decreased OT-LTD in

adulthood. Moreover, because dopamine-dependent[25] cocaine CPP behaviour (Fig. 2g–j, Extended Data Fig. 4) is maintained across development, these results indicate that the closure of the critical period for social reward learning requires selective regulation of OT signalling mechanisms.

The current studies also provide the first direct evidence, to our knowledge, to link the prosocial effects of MDMA[10] with metaplastic changes in OT-LTD (Fig. 3n–p), as well as synaptic and behavioural effects that require activation of OT receptors in the NAc (Fig. 4). We are aware of no evidence that MDMA binds to OT receptors. Instead, our results (Extended Data Fig. 6) are consistent with previous reports that MDMA binds to SERT[12] and triggers OT release[7–9] through activation of 5HT4 receptors on OT neurons[15]. These results add to growing evidence[26,27] that the 5HT4 receptor is a regulator of presynaptic neurotransmitter release. Extended Data Fig. 10 shows our working model. Notably, our proposed mechanism of metaplastic upregulation of OT

signalling mechanisms parallels previous observations of acetylcholine receptor upregulation following nicotine administration[28].

Finally, mechanistic insights into the reopening of the critical period for social reward learning may inform the development of novel therapeutic agents. Indeed, on the basis of its safety and efficacy profile, MDMA-assisted psychotherapy for post-traumatic stress disorder (PTSD) has been designated a 'Breakthrough Therapy' by the FDA, and phase III trials are currently underway[29]. Despite the excitement over these clinical findings, the mechanisms that underlie the therapeutic efficacy of MDMA for PTSD are largely unknown. Some have proposed that these results are the consequence of the ability of MDMA to induce memory reconsolidation and fear extinction[29,30]. Alternatively, our results indicate that the therapeutic effects of MDMA share a number of features with MDMA-induced reopening of the critical period for social reward learning, including: rapid onset (Extended Data Fig. 7k–r); durability beyond the acute effects of the drug (Extended Data Fig. 7k–r); and dependence on social setting (Extended Data Fig. 7f–j). These similarities suggest that the therapeutic efficacy of MDMA might stem from its ability to reopen the critical period for social reward learning, thereby fostering the alliance between psychologist and patient during MDMA-assisted psychotherapy.

Online content

Any methods, additional references, Nature Research reporting summaries, source data, statements of data availability and associated accession codes are available at https://doi.org/10.1038/s41586-019-1075-9.

1. Hübener, M. & Bonhoeffer, T. Neuronal plasticity: beyond the critical period. *Cell* **159**, 727–737 (2014).
2. Patton, M. H., Blundon, J. A. & Zakharenko, S. S. Rejuvenation of plasticity in the brain: opening the critical period. *Curr. Opin. Neurobiol.* **54**, 83–89 (2019).
3. Yazar-Klosinski, B. B. & Mithoefer, M. C. Potential psychiatric uses for MDMA. *Clin. Pharmacol. Ther.* **101**, 194–196 (2017).
4. Dölen, G., Darvishzadeh, A., Huang, K. W. & Malenka, R. C. Social reward requires coordinated activity of nucleus accumbens oxytocin and serotonin. *Nature* **501**, 179–184 (2013).
5. McEwen, B. B. Brain-fluid barriers: relevance for theoretical controversies regarding vasopressin and oxytocin memory research. *Adv. Pharmacol.* **50**, 531–592, 655–708 (2004).
6. Lee, M. R. et al. Oxytocin by intranasal and intravenous routes reaches the cerebrospinal fluid in rhesus macaques: determination using a novel oxytocin assay. *Mol. Psychiatry* **23**, 115–122 (2018).
7. Thompson, M. R., Callaghan, P. D., Hunt, G. E., Cornish, J. L. & McGregor, I. S. A role for oxytocin and 5-HT(1A) receptors in the prosocial effects of 3,4 methylenedioxymethamphetamine ("ecstasy"). *Neuroscience* **146**, 509–514 (2007).
8. Hunt, G. E., McGregor, I. S., Cornish, J. L. & Callaghan, P. D. MDMA-induced c-Fos expression in oxytocin-containing neurons is blocked by pretreatment with the 5-HT-1A receptor antagonist WAY 100635. *Brain Res. Bull.* **86**, 65–73 (2011).
9. Forsling, M. L. et al. The effect of 3,4-methylenedioxymethamphetamine (MDMA, 'ecstasy') and its metabolites on neurohypophysial hormone release from the isolated rat hypothalamus. *Br. J. Pharmacol.* **135**, 649–656 (2002).
10. Shulgin, A. A. T. & Nichols, D. E. Characterization of three new psychotomimetics. *Psychopharmacol. Hallucinog.* **2**, 74–83 (1978).
11. Rudnick, G. & Wall, S. C. The molecular mechanism of "ecstasy" [3,4-methylenedioxy-methamphetamine (MDMA)]: serotonin transporters are targets for MDMA-induced serotonin release. *Proc. Natl Acad. Sci. USA* **89**, 1817–1821 (1992).
12. Field, J. R., Henry, L. K. & Blakely, R. D. Transmembrane domain 6 of the human serotonin transporter contributes to an aqueously accessible binding pocket for serotonin and the psychostimulant 3,4-methylene dioxymethamphetamine. *J. Biol. Chem.* **285**, 11270–11280 (2010).
13. Edsinger, E. & Dölen, G. A conserved role for serotonergic neurotransmission in mediating social behavior in octopus. *Curr. Biol.* **28**, 3136–3142.e4 (2018).
14. Simmler, L. D. et al. Pharmacological characterization of designer cathinones in vitro. *Br. J. Pharmacol.* **168**, 458–470 (2013).
15. Jørgensen, H., Riis, M., Knigge, U., Kjaer, A. & Warberg, J. Serotonin receptors involved in vasopressin and oxytocin secretion. *J. Neuroendocrinol.* **15**, 242–249 (2003).
16. Trigo, J. M. et al. 3,4-Methylenedioxymethamphetamine self-administration is abolished in serotonin transporter knockout mice. *Biol. Psychiatry* **62**, 669–679 (2007).
17. Abraham, W. C. & Bear, M. F. Metaplasticity: the plasticity of synaptic plasticity. *Trends Neurosci.* **19**, 126–130 (1996).
18. Klapoetke, N. C. et al. Independent optical excitation of distinct neural populations. *Nat. Methods* **11**, 338–346 (2014).
19. Blakemore, S.-J. & Mills, K. L. Is adolescence a sensitive period for sociocultural processing? *Annu. Rev. Psychol.* **65**, 187–207 (2014).
20. Nelson, E. E., Jarcho, J. M. & Guyer, A. E. Social re-orientation and brain development: an expanded and updated view. *Dev. Cogn. Neurosci.* **17**, 118–127 (2016).
21. Pedersen, C. A. Biological aspects of social bonding and the roots of human violence. *Ann. NY Acad. Sci.* **1036**, 106–127 (2004).
22. Leung, R. K., Toumbourou, J. W. & Hemphill, S. A. The effect of peer influence and selection processes on adolescent alcohol use: a systematic review of longitudinal studies. *Health Psychol. Rev.* **8**, 426–457 (2014).
23. Nicolaisen, M. & Thorsen, K. Who are lonely? Loneliness in different age groups (18–81 years old), using two measures of loneliness. *Int. J. Aging Hum. Dev.* **78**, 229–257 (2014).
24. Shapiro, L. E. & Insel, T. R. Ontogeny of oxytocin receptors in rat forebrain: a quantitative study. *Synapse* **4**, 259–266 (1989).
25. Lüscher, C. & Malenka, R. C. Drug-evoked synaptic plasticity in addiction: from molecular changes to circuit remodeling. *Neuron* **69**, 650–663 (2011).
26. Nair, S. G. & Gudelsky, G. A. 3,4-Methylenedioxymethamphetamine (MDMA) enhances the release of acetylcholine by 5-HT4 and D1 receptor mechanisms in the rat prefrontal cortex. *Synapse* **58**, 229–235 (2005).
27. Hagena, H. & Manahan-Vaughan, D. The serotonergic 5-HT4 receptor: A unique modulator of hippocampal synaptic information processing and cognition. *Neurobiol. Learn. Mem.* **138**, 145–153 (2017).
28. Melroy-Greif, W. E., Stitzel, J. A. & Ehringer, M. A. Nicotinic acetylcholine receptors: upregulation, age-related effects and associations with drug use. *Genes Brain Behav.* **15**, 89–107 (2016).
29. Mithoefer, M. C. et al. 3,4-Methylenedioxymethamphetamine (MDMA)-assisted psychotherapy for post-traumatic stress disorder in military veterans, firefighters, and police officers: a randomised, double-blind, dose-response, phase 2 clinical trial. *Lancet Psychiatry* **5**, 486–497 (2018).
30. Young, M. B. et al. Inhibition of serotonin transporters disrupts the enhancement of fear memory extinction by 3,4-methylenedioxymethamphetamine (MDMA). *Psychopharmacology (Berl.)* **234**, 2883–2895 (2017).

Author contributions G.D. and R.N. designed the study, interpreted results and wrote the paper. R.N. performed and analysed behavioural experiments, electrophysiology and optogenetics. R.N., E.M.L. and R.R. performed stereotaxic injections, performed and analysed immunohistochemistry experiments. R.N. and E.M.L. validated Chronos function in OT neurons. G.D. designed the OT-2A-Flp KI mouse construct. A.Y., R.X. and E.B. designed the AAV-CAG-FonChronos-TdTomato viral construct. All authors edited the paper.

Competing interests The authors declare no competing interests.

Additional information
Extended data is available for this paper at https://doi.org/10.1038/s41586-019-1075-9.
Supplementary information is available for this paper at https://doi.org/10.1038/s41586-019-1075-9.
Reprints and permissions information is available at http://www.nature.com/reprints.
Correspondence and requests for materials should be addressed to G.D.
Publisher's note: Springer Nature remains neutral with regard to jurisdictional claims in published maps and institutional affiliations.

METHODS

Mice. Male and female C57BL/6 mice were bred in-house and weaned or delivered from Jackson Laboratory (stock # 00664) at 3 weeks of age. All experiments were performed in males except Extended Data Fig. 1. Oxytocin-2A-Flp optimized knock-in (OT-2A-Flp KI) mice were generated by Cyagen Biosciences (Santa Clara, CA) according to our design. Similar to the strategy employed by the oxytocin-IRES-Cre knock-in mouse[31] we replaced the stop codon in exon 3 of the endogenous oxytocin gene (*Oxt*) with a 2A-Flp construct. The co-translational cleavage 2A peptide strategy (known to have more robust expression of its downstream gene than the internal ribosome entry site (IRES) strategy[32,33]) was used to separate Flp and OT, because Flp is directed to the nucleus, while OT is directed to the cytoplasm. Flp-dependent GFP reporter mice (Stock # 32038; Swiss Webster background) were obtained from the Mutant Mouse Resource Center. Transgenic mice were bred in-house and were weaned at 3 weeks of age. All mice other than GFP reporter mice were kept on a C57BL/6 background and all mice were maintained on a 12 h:12 h natural light–dark cycle, starting at 8:30 a.m. with food and water provided ad libitum. All behavioural experiments were conducted during the same circadian period (8:30am to 8:30pm) in a dedicated, sound and odour-controlled behavioural testing room, which is separated from the vivarium, and no other experiments were conducted simultaneously in the same room. Sample size was estimated based on previous work and published literature. Experimenters were blinded to the treatment condition when subjective criteria were used as a component of data analysis, and control and test conditions were interleaved for all experiments. Mice were randomly assigned to experimental and control groups. All procedures complied with the animal care standards set forth by the National Institutes of Health and were in accordance with protocols approved by the Johns Hopkins University Animal Care and Use Committee.

Social CPP. The protocol for social CPP was adapted from previously published work[4,34,35]. Upon weaning, animals were socially housed (4–5 same sex cage mates, unless otherwise specified) in a cage containing corncob bedding (Anderson Cob, 1/4" cob, Animal Specialties and Provisions) until the pre-determined age for social CPP testing. Each animal was used at only one behavioural time point. At the pre-determined age, animals were placed in an open field activity chamber (ENV-510, Med Associates) equipped with infrared beams and a software interface (Activity Monitor, Med Associates) to monitor the position of the mouse. The apparatus was partitioned into two equally sized zones using a clear Plexiglas wall, with a 5-cm diameter circular hole at the base; each zone contained one type of novel bedding (Alpha-Dri, Animal Specialties and Provisions or Kaytee Soft Granule, Petco). The amount of time spent freely exploring each zone was recorded during 30-min test sessions. After an initial pre-conditioning trial to establish baseline preference for the two sets of bedding cues, mice were assigned to receive social conditioning with cage mates for 24 h on one type of bedding, followed by 24 h of isolation conditioning (without cage mates) on the other bedding. To assure unbiased design, chamber assignments were counterbalanced for side and bedding cues. Immediately after the isolation conditioning, a 30-min post-conditioning trial was conducted to establish preference for the two conditioned cues. CPP is a learned association between a condition (for example, social, cocaine) and a cue (bedding). It does not require scent from other mice, as the bedding itself serves as the cue. This assay does not measure the quality of social interactions, but the magnitude of the reward learning is almost certainly linked to changes in the types of social interactions animals engage in as they mature (for example, decreased play behaviour, increased agonistic behaviour). Unlike drug rewards, which are non-contingently rewarding, natural rewards, including water, food, and social interactions, are state-dependent, and require that the animal be thirsty, hungry, or lonely. Consistent with this observation, previous studies have shown that in order for social CPP to be expressed, the animals must either (1) undergo 1 week of social isolation before conditioning or 2) experience the isolation phase of conditioning immediately before the post-conditioning trial. We elected to use the second protocol because it simplified our experimental design, especially for molecular manipulations that require 1 week for full expression of viruses.

Exclusion criteria for this behaviour were strictly defined as a pre-conditioning preference score of >1.5 or <0.5. Animals were never excluded based on the quality of their social interactions; furthermore, because these animals have been housed together since weaning, aggressive interactions were extremely rare, even in adults. Pre-conditioning versus post-conditioning social preference scores were considered significant if paired student's *t*-test *P* values were <0.05. Comparisons between experimental conditions were made using both normalized social preference scores (time spent in social zone post divided by pre), and subtracted social preference scores (time spent in social zone post minus pre); these were considered significant if unpaired student's *t*-test (two conditions), or ANOVA (more than two conditions; Fig. 1 and Extended Data Fig. 1) *P* values were <0.05, and Bonferroni corrected *P* values were <0.0036. Although the convention in the field is to refer to this assay as a measure of social reward[36], the assay actually measures the contribution of both social preference and isolation aversion[35]. In pilot experiments,

we corroborated these findings, and determined that comparisons between the socially-conditioned cue and the isolation-conditioned cue improve the robustness of the two-day protocol and therefore the scalability of this assay. All experiments were performed during the mouse rest period (light cycle), as pilot experiments revealed that social CPP is most robust if assayed during this period. Prior to intraperitoneal (i.p.) drug treatment experiments (MDMA, OT, oxytocin receptor antagonists (OTR-A or L-368,899 hydrochloride), cocaine, or saline), animals were habituated to the injection procedure by daily i.p. injections of saline in the home cage for 3 days. Pharmacological delivery schedules were counterbalanced for type of drug. Unless otherwise stated, for MDMA pretreatment experiments animals were tested 48 h after the injection to allow for complete clearance of MDMA and its metabolites[9]. For the experiment testing involvement of the social context on the effect of MDMA, the injection of MDMA was followed by 3 h in either the isolate or social condition, after which time the animals were brought back to their home cages with their cage mates for 2 days before testing for social CPP.

Cocaine CPP. For cocaine CPP, experiments were performed in the same open field activity chambers as social CPP using an identical configuration. After 3 days of habituation to i.p. saline injections in the home cage, the amount of time spent exploring each zone of the activity chamber during a 30-min pre-conditioning test was measured. After 24 h, mice were randomly assigned in a counterbalanced fashion to receive an i.p. injection of cocaine (20 mg/kg (Fig. 2g–j, Extended Data Fig. 7 s–v), 10 mg/kg (Extended Data Fig. 4) or 5 mg/kg (Extended Data Fig. 4)) immediately followed by 30 min conditioning on one bedding (Soft Granule or Alpha Dri). A second 30-min conditioning session was conducted 24 h later on the other bedding after an i.p. injection of saline (equal volume to cocaine). A 30 min post-conditioning test session was conducted 24 h later to determine each mouse's preference for the cocaine versus saline associated beddings. The time course of social CPP and cocaine CPP are slightly different, as social CPP is performed immediately after the non-social pairing, whereas cocaine CPP is performed 24 h after conditioning. Analyses were conducted and significance determined as for social CPP. Pharmacological delivery schedules were counterbalanced for the type of drug (that is, saline, cocaine or MDMA).

Electrophysiology. Parasagittal slices (250 μm thick) containing the NAc core were prepared from C57BL/6 mice using standard procedures. In brief, after mice were anaesthetized with isoflurane and decapitated, brains were quickly removed and placed in ice-cold low-sodium, high-sucrose dissecting solution (228 mM sucrose, 26 mM $NaHCO_3$, 11 mM glucose, 2.5 mM KCl, 1 mM NaH_2PO_4, 1 mM $MgSO_4$, 0.5 mM $CaCl_2$). Slices were cut by adhering the two sagittal hemispheres containing the NAc core to the stage of a Leica vibroslicer. Slices were allowed to recover for a minimum of 60 min in a submerged holding chamber (~25 °C) containing artificial cerebrospinal fluid (ACSF) consisting of 119 mM NaCl, 2.5 mM KCl, 2.5 mM $CaCl_2$, 1.3 mM $MgSO_4$, 1 mM NaH_2PO_4, 11 mM glucose and 26.2 mM $NaHCO_3$. Slices were then removed from the holding chamber and placed into the recording chamber, where they were continuously perfused with oxygenated (95% O_2, 5% CO_2) ACSF at 2 ml/min at 25 °C. To isolate EPSCs, picrotoxin (50 μM, Sigma) was added to the ACSF to block $GABA_A$ receptor-mediated inhibitory synaptic currents. Whole-cell voltage-clamp recordings from MSNs were obtained under visual control using a 40× objective. The NAc core was identified by the presence of the anterior commissure. Recordings were made with electrodes (2.5–3.5 MΩ) filled with 115 mM $CsMeSO_4$, 20 mM CsCl, 10 mM HEPES, 0.6 mM EGTA, 2.5 mM $MgCl$, 10 mM Na-phosphocreatine, 4 mM Na-ATP, 0.3 mM Na-GTP, and 1 mM QX-314. Excitatory afferents were stimulated with a bipolar nichrome wire electrode placed at the border between the NAc core and cortex dorsal to the anterior commissure. Recordings were performed using a Multiclamp 700B (Molecular Devices), filtered at 2 kHz and digitized at 10 kHz. EPSCs were evoked at a frequency of 0.1 Hz while MSNs were voltage-clamped at −70 mV. Data acquisition and analysis were performed on-line using custom Igor Pro software. Input resistance and access resistance were monitored continuously and experiments were terminated with a change >15%.

Summary LTD graphs were generated by averaging the peak amplitudes of individual EPSCs in 1-min bins (6 consecutive sweeps) and normalizing these to the mean value of EPSCs collected during the 10-min baseline immediately before the LTD-induction protocol. Individual experiments were then averaged together. As described previously[4,37], all experimental drugs (OT, 1 μM, Tocris Biosciences; CP-93129 dihydrochloride, 2 μM, Tocris Biosciences; MDMA, 2 μM, NIDA, Drug supply program) were bath applied for 10 min following the collection of baseline data to test their ability to induce LTD. For experiments examining the blockade of MDMA-LTD or OT-LTD (Fig. 4a–c, Extended Data Fig. 6), slices were pre-incubated in antagonist (OTR-A, 5 μM L-368,899 hydrochloride; serotonin transporter (SERT) antagonist, fluoxetine hydrochloride, 10 μM; 5HTR4 antagonist, SB203186 hydrochloride, 10 μM; 5HTR1a antagonist, WAY 100635 maleate, 10 nM or 10 μM, Tocris Biosciences) for at least 30 min before recording. For experiments examining the occlusion of MDMA-LTD, after stabilization of OT-LTD (at 60 min post induction), 2 μM MDMA was bath applied for 10 min.

Comparisons between experimental manipulations were made using a two-tailed, unpaired Students t-test with $P < 0.05$ considered significant. All values are reported as mean ± s.e.m.

To confirm the functional efficiency of Chronos expressed in OT cells, coronal slices containing the PVN (250 μm) were prepared in a manner similar to that described above. After at least 60 min recovery, slices were transferred to the recording chamber and Chronos-expressing OT cells were visually targeted for recording based on TdTomato fluorescence. Recordings were conducted in current clamp using patch pipettes (2–4 MΩ) filled with internal solution containing 130 mM K-gluconate, 10 mM HEPES, 1 mM NaCl, 1 mM CaCl₂, 10 mM EGTA, 1 mM MgCl, 2 mM Mg-ATP, 0.5 mM Na-GTP and 0.125% neurobiotin. As PVN OT neurons are often spontaneously active, a small amount of hyperpolarizing current (about −20 pA) was injected to eliminate spontaneous action potentials and facilitate analysis. Optical stimulation (470 nm; 5 ms; 20 pulses) was delivered through the 40× microscope objective at 10, 20 and 40 Hz. Data were acquired and analysed using the Recording Artist plugin in Igor Pro.

For the miniature EPSC experiments, slices prepared from OT-2A-Flp KI mice injected with AAV-CAG-_Fon_Chronos-TdTomato were optically stimulated for 30 min through the 40× microscope objective (5 ms pulse, 20 Hz, 15 mW, 470 nm) in the presence or absence of OTR-A (5 μM, L-368,899 hydrochloride, Tocris Biosciences) before mEPSCs were recorded. Miniature EPSCs were collected from 0–6 h after photostimulation at a holding potential of −70 mV in the presence of tetrodotoxin (TTX) (0.5 μM, Tocris Biosciences) and picrotoxin (50 μM, Sigma). Two minutes after break-in, 30-s blocks of events (total of 200 events per cell) were acquired and analysed using custom Igor Pro software with threshold parameters set at 5 pA amplitude and <3 ms rise time. All events included in the final data analysis were verified visually.

Virus generation. The pAAV-CAG-_Fon_Chronos-TdTomato construct (deposited on Addgene, accession number 105834) was assembled using seamless cloning by Epoch Life Science, cloning the Chronos-TdTomato gene into a pAAV-CAG-_Fon_ backbone at the NheI and AscI sites. The gene is expressed under the CAG promoter and flanked by Flp recombination sequences FRT and F5 separated with a 50-bp spacer. The subsequent AAV virus was packaged in serotype 2/8 by the UNC vector core via co-transfection of AAV293 cells with pHelper, pAAV rep2/cap8 and pAAV-CAG-_Fon_Chronos-TdTomato at 1:1:1. The cell pellets were re-suspended in the AAV lysis buffer and freeze–thawed three times. Supernatants were collected and then gradient ultracentrifugation and dialysis were performed.

Stereotaxic injection. Stereotaxic injection of AAV-CAG-_Fon_Chronos-TdTomato into the PVN of C57BL/6 wild-type WT and OT-2A-Flp KI mice was performed at P33 under general ketamine–medetomidine anaesthesia using a stereotaxic instrument (David Kopf). A small volume (∼1 μl) of concentrated virus solution was injected bilaterally into the PVN (bregma −0.6 mm; lateral 0.35 mm; ventral −5.1 mm), at a slow rate (100 nl/min) using a syringe pump (Harvard Apparatus, MA). The injection needle was withdrawn 10 min after the end of the infusion. Following virus injection, animals were housed as dyad pairs. Injection sites and viral infectivity were confirmed post-hoc by preparing sections (50 μm) containing the PVN. Robust TdTomato expression was observed throughout the rostral–caudal extent of the PVN in all animals.

Stereotaxic injection of Retrobeads (RtBs) into the nucleus accumbens (NAc) was performed under general ketamine–medetomidine anaesthesia using a stereotaxic instrument (David Kopf). A small volume (∼30 nl) of diluted RtB solution (1:4) was injected unilaterally into the NAc core (bregma 1.54 mm; lateral 1.06 mm; ventral 4.1 mm), at a slow rate (20 nl/min) using a syringe pump (Harvard Apparatus, MA). The injection needle was withdrawn 10 min after the end of the infusion. Injection sites were confirmed post-hoc by preparing sections (20–50 μm) containing the NAc. Following RtB injection, the animals were returned to their home cages for one week before intracardial perfusion.

Fibre implantation. Two months after virus injection, optic fibre cannulas were implanted bilaterally above the NAc (bregma 1.6 mm; lateral 1.1 mm; ventral −3.95 mm) under general ketamine–medetomidine anaesthesia using a stereotaxic instrument (David Kopf). The cannulas were made in-house using 1.25 mm diameter multimode ceramic ferrule, 200 μm fibre optic cable (NA 0.53) and epoxy. Cannulas were secured to the skull using miniature screws (thread size 00-90 × 1/16) and dental adhesive cement.

Optogenetics. For optogenetic photostimulation, the fibre optic cannulas were connected to a 473-nm laser diode through a FC/PC adaptor and a fibre optic 1 × 2 rotary joint. Laser output was controlled using a pulse generator (Master-8), which delivered 5-ms light pulses at 20 Hz. Light output through the optical fibres was adjusted to 20 mW using a digital power-meter console. Each member of the dyad received 30 min simultaneous optical stimulation (5 ms pulse, 20 Hz, 20 mW) in a chamber divided by a perforated grid, which provided partial access to social cues (visual, olfactory, auditory), and the animals were tested for social CPP 48 h later, at P98. Following behavioural testing, viral expression, OT neuronal specificity, and fibre placement were confirmed for each animal (Extended Data

Fig. 9e–h, j). Notably, dyad housing alone had no effect on the magnitude of social CPP (Extended Data Fig. 11).

Infusion cannula implantation and microinjection. Standard stereotaxic procedures were used to implant guide cannulas under ketamine–dexmedetomidine anaesthesia. In brief, at P91, double cannula guides (C235GS, 26GA, C/C distance 2.0 mm, 5 mm pedestal, cut 4 mm below pedestal, custom specified for mouse bilateral NAc coordinates, Plastics One Inc.) were implanted above the NAc of male mice following bilateral craniotomy (bregma 1.6 mm; lateral 1.0 mm) and attached to the skull using dental acrylic. A third hole was drilled a few mm posterior to the guide cannula holes; this hole was enlarged for placement of an anchor screw. After recovery, all animals were returned to their home cage and given free access to food and water.

One week after cannula implantation, and 2 days before social CPP testing, mice were microinjected with MDMA (11 μM) with or without OTR-A (L-368,899, 500 ng) into the NAc. Immediately before microinjection, a 33-gauge injector cannula that protruded 1.6 mm below the guide cannula and was connected to a syringe pump (Harvard Apparatus, MA) was inserted into the guide cannula. Microinjections were delivered at a rate of 1 μl/min, with a total injection volume of 1 μl. Injector cannulas remained in place for an additional minute before being removed. After infusion the mice were put back into their home cage for 2 days before the social CPP. Cannula placement was verified by post-hoc histology.

Histology and immunohistochemistry. After transcardial perfusion with phosphate buffered saline (PBS (pH 7.4, 1 M)) followed by 10% formalin, brains were post-fixed overnight in formalin at 4 °C and transferred to PBS. Coronal sections of the PVN (20 μm) and the NAc (50 μm) were cut in PBS using a vibratome. For experiments in which fluorescent colocalization was analysed, serial brain sections (20 μm thickness) were cut using a cryostat following cryoprotection of tissue with a 30% sucrose solution containing 0.01% sodium azide. Sections were mounted on slides in PBS and allowed to dry. Subsequently, sections were rinsed four times for 10 min each and blocked with 10% normal horse serum (NHS) and 2% bovine serum albumin (BSA) in PBS/0.5% triton-X100 (PBST). To label OT neurons immunohistochemically, the anti-OT-neurophysin antibody PS38 was used[38,39] (gift from H. Gainer; 1:150). The PVN or NAc was stained for OT in 1% NHS in PBST at room temperature (RT) overnight. Sections were rinsed four times for 10 min each in PBS followed by 2 h secondary antibody stain using either Alexa 350 (RtB or Tdtomato colocalization; Life Technologies; goat anti-mouse; 1:200) or Alexa 647 (GFP colocalization; Life Technologies; goat anti-mouse; 1:1,000 in 1% NHS in PBST) at RT. Sections were then rinsed four times for 10 min at RT and stained with DAPI (diluted 1:5,000 in PBS) and the slides were coverslipped. Images were acquired using an EVOS or Olympus BX41 microscope with 4×, 10× and 40× objectives or a Zeiss LSM880 confocal microscope using a 63× objective. Images were analysed using ImageJ.

Genotyping. Oxytocin-2A-Flp optimized knock-in mice (OT-2A-Flp KI) were genotyped before weaning using polymerase chain reaction (PCR) analysis of DNA isolated from tail snips. The wild-type allele was identified by a 622-bp PCR product and the mutant allele by a 308-bp PCR product using the following primers: *mOxtR1*: TCCGACAATTAGACACCAGTCAA; *mOxtF1*: CTACCTGAGCAGCTACATCAACAG; *mOxtF2*: AGGGCTTTGGGAAGTG TTAGGCT.

The reactions were run under the following conditions: 94 °C × 3 min, (94 °C × 30 s, 60 °C × 35 s, 72 °C × 35 s) × 38 cycles, 72 °C × 5 min. For OT-2A-Flp::FonGFP mice, in addition to the genotyping for OT-2A-Flp, the wild-type allele was identified by a 603-bp PCR product, and the FonGFP allele by a 320-bp PCR product using the following primers; mutant: CCAGGCGGGCCATTTACCGTAAG; common: AAAGTCGCTCTGAGTTGTTAT; wild-type: GGAGCGGGAGAAATGGATATG. The reactions were run using the Gt(ROSA)26Sortm(CAG) protocol published by Jackson Laboratories.

Statistics. Comparisons between experimental manipulations were made using a two-tailed Students t-test (paired or unpaired, as appropriate), ANOVA for repeated measures, and MANOVA for comparisons between multiple outcome measures, with $P < 0.05$ considered significant. Homogeneity of variance was tested using Levene's test for equality of variances and normality was tested using the Shapiro–Wilk test of normality using SPSS; post-hoc tests were carried out only if global measures were significant.

Reporting summary. Further information on research design is available in the Nature Research Reporting Summary linked to this paper.

Data availability

The pAAV-CAG-_Fon_Chronos-TdTomato construct has been deposited on Addgene (accession number 105834). Oxytocin-2A-Flp optimized knock-in mice, and data sets are available from the corresponding author upon request.

31. Wu, Z. et al. An obligate role of oxytocin neurons in diet induced energy expenditure. *PLoS One* **7**, e45167 (2012).

32. Furler, S., Paterna, J. C., Weibel, M. & Büeler, H. Recombinant AAV vectors containing the foot and mouth disease virus 2A sequence confer efficient bicistronic gene expression in cultured cells and rat substantia nigra neurons. *Gene Ther.* **8**, 864–873 (2001).
33. Chan, H. Y. et al. Comparison of IRES and F2A-based locus-specific multicistronic expression in stable mouse lines. *PLoS One* **6**, e28885 (2011).
34. Douglas, L. A., Varlinskaya, E. I. & Spear, L. P. Rewarding properties of social interactions in adolescent and adult male and female rats: impact of social versus isolate housing of subjects and partners. *Dev. Psychobiol.* **45**, 153–162 (2004).
35. Panksepp, J. B. & Lahvis, G. P. Social reward among juvenile mice. *Genes Brain Behav.* **6**, 661–671 (2007).
36. Silverman, J. L., Yang, M., Lord, C. & Crawley, J. N. Behavioural phenotyping assays for mouse models of autism. *Nat. Rev. Neurosci.* **11**, 490–502 (2010).
37. Mathur, B. N., Capik, N. A., Alvarez, V. A. & Lovinger, D. M. Serotonin induces long-term depression at corticostriatal synapses. *J. Neurosci.* **31**, 7402–7411 (2011).
38. Whitnall, M. H., Key, S., Ben-Barak, Y., Ozato, K. & Gainer, H. Neurophysin in the hypothalamo-neurohypophysial system. II. Immunocytochemical studies of the ontogeny of oxytocinergic and vasopressinergic neurons. *J. Neurosci.* **5**, 98–109 (1985).
39. Ben-Barak, Y., Russell, J. T., Whitnall, M. H., Ozato, K. & Gainer, H. Neurophysin in the hypothalamo-neurohypophysial system. I. Production and characterization of monoclonal antibodies. *J. Neurosci.* **5**, 81–97 (1985).
40. Dölen, G. Oxytocin: parallel processing in the social brain? *J. Neuroendocrinol.* **27**, 516–535 (2015).
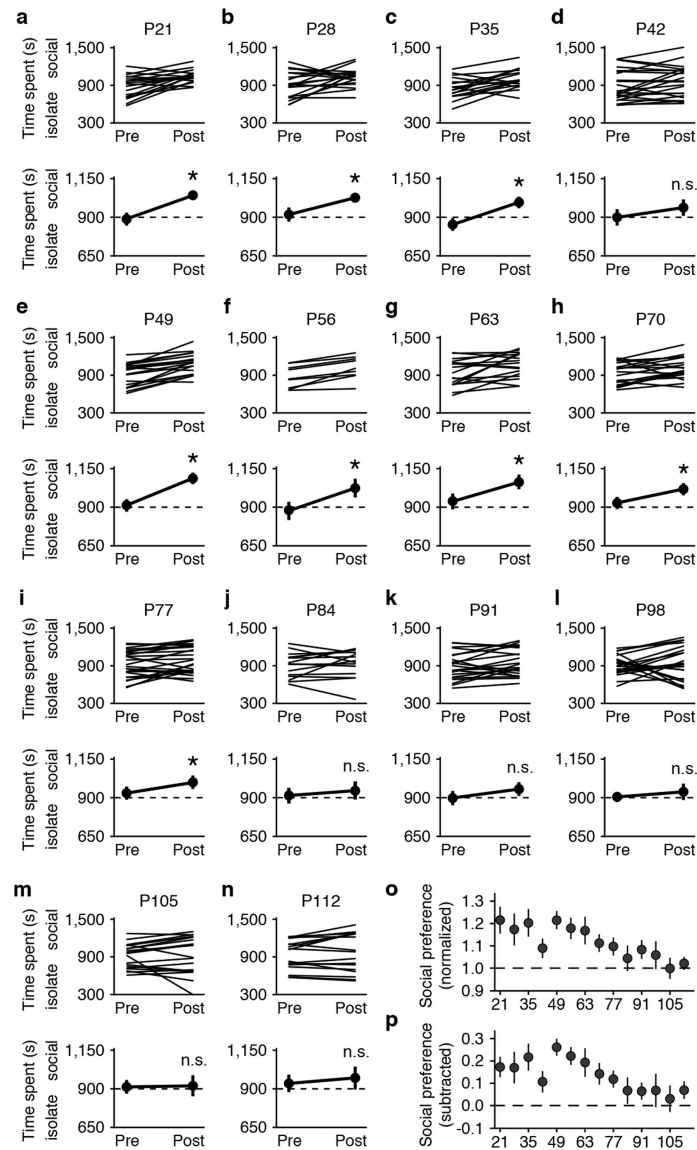
Extended Data Fig. 1 | Social reward learning is constrained by a critical period in female mice. a–n, Individual (top) and average (bottom) responses of female mice from P21 to P112. **o**, Comparison across ages using the normalized social preference score reveals a developmental decline in the magnitude of social CPP in females. One-way ANOVA ($F_{(13,248)} = 1.867$, $P = 0.034$). P21, $n = 13$; $t_{(12)} = -3.146$, $P = 0.008$; P28, $n = 20$; $t_{(19)} = -2.097$, $P = 0.049$; P35, $n = 17$; $t_{(16)} = -3.226$, $P = 0.005$; P42, $n = 22$; $t_{(21)} = -1.773$, $P = 0.910$; P49, $n = 19$; $t_{(18)} = -6.35$, $P \leq$ 0.001; P56, $n = 9$; $t_{(8)} = -4.938$, $P = 0.001$; P63, $n = 17$; $t_{(16)} = -2.659$,

$P = 0.017$; P70, $n = 19$; $t_{(18)} = -2.51$, $P = 0.022$; P77, $n = 25$; $t_{(24)} = -2.551$, $P = 0.018$; P84, $n = 15$; $t_{(14)} = -0.777$, $P = 0.45$; P91, $n = 18$; $t_{(17)} = -2.027$, $P = 0.059$; P98, $n = 23$; $t_{(22)} = -0.62$, $P = 0.5420$; P105, $n = 19$; $t_{(18)} = -0.155$, $P = 0.8790$; P112, $n = 17$; $t_{(16)} = -1.223$, $P = 0.2390$; n is the number of mice; two-tailed paired t-test pre versus post. **p**, Comparison across ages using the subtracted social preference score reveals a similar trend. One-way ANOVA ($F_{(13,248)} = 1.625$, $P = 0.079$). Data are presented as mean ± s.e.m. *$P < 0.05$; n.s., comparisons not significant ($P > 0.05$).
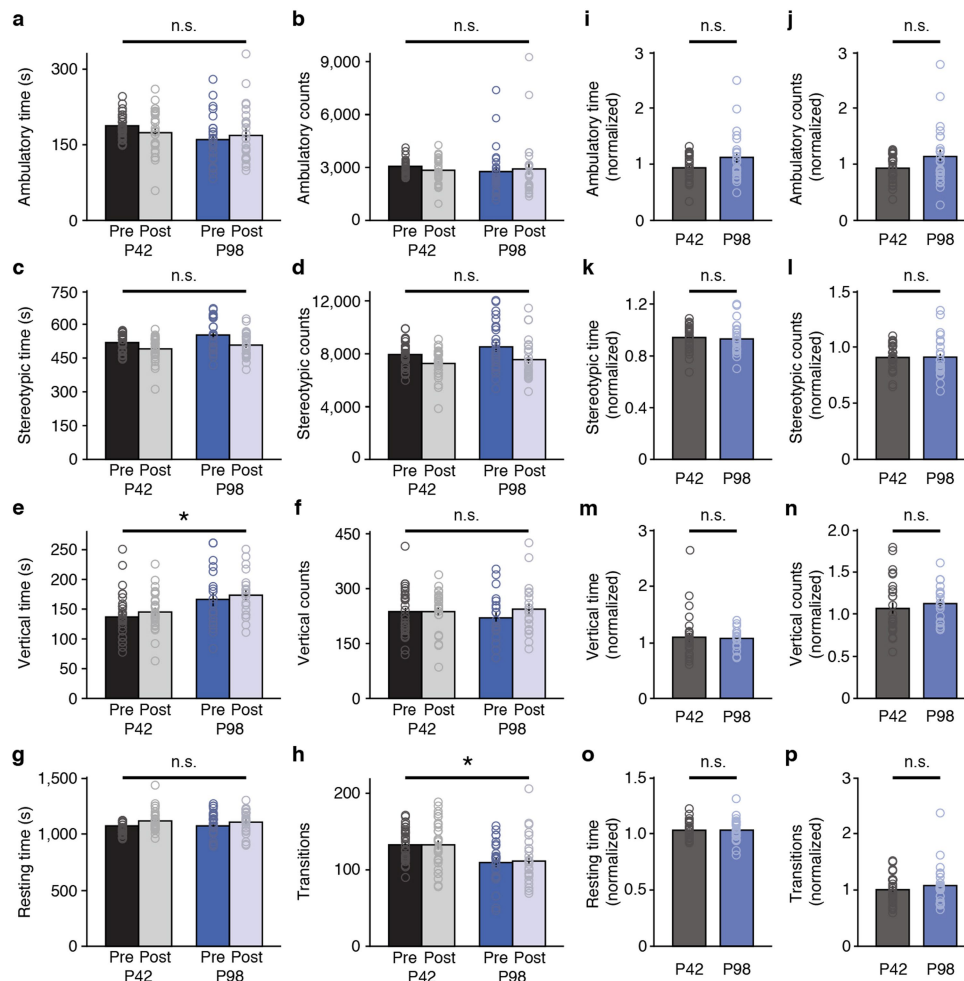
Extended Data Fig. 2 | Locomotor activity during social CPP is similar in juvenile and adult mice. a–h, MANOVA ($F_{(8,36)} = 8.022$, $P < 0.001$). Ambulatory time ($F_{(1,43)} = 2.234$, $P = 0.142$) (**a**), ambulatory counts ($F_{(1,43)} = 0.030$, $P = 0.864$) (**b**), stereotypic time ($F_{(1,43)} = 1.659$, $P = 0.205$) (**c**), stereotypic counts ($F_{(1,43)} = 0.497$, $P = 0.485$) (**d**), vertical counts ($F_{(1,43)} = 0.077$, $P = 0.783$) (**f**) and resting time ($F_{(1,43)} = 0.023$, $P = 0.879$) (**g**) are not different between P42 ($n = 26$ animals) and P98 ($n = 19$ animals). Vertical time (**e**) is increased ($F_{(1,43)} = 6.803$, $P = 0.012$) and number of transitions (**h**) is decreased ($F_{(1,43)} = 12.418$, $P = 0.001$) in adult compared to juvenile mice. **i–p**, None of the eight variables normalized (post/pre) are different between P42 and P98 (MANOVA ($F_{(8,36)} = 3.174$, $P = 0.008$); normalized ambulatory time ($F_{(1,43)} = 3.443$, $P = 0.070$) (**i**), normalized ambulatory counts ($F_{(1,43)} = 3.937$, $P = 0.054$) (**j**), normalized stereotypic time ($F_{(1,43)} = 0.610$, $P = 0.439$) (**k**), normalized stereotypic counts ($F_{(1,43)} = 0.086$, $P = 0.771$) (**l**), normalized vertical time ($F_{(1,43)} = 0.071$, $P = 0.791$) (**m**), normalized vertical counts ($F_{(1,43)} = 0.441$, $P = 0.510$) (**n**), normalized resting time ($F_{(1,43)} = 0.077$, $P = 0.783$) (**o**) and normalized number of transitions ($F_{(1,43)} = 0.279$, $P = 0.600$) (**p**). Data are presented as mean ± s.e.m. *$P < 0.05$; n.s., comparisons not significant ($P > 0.05$).
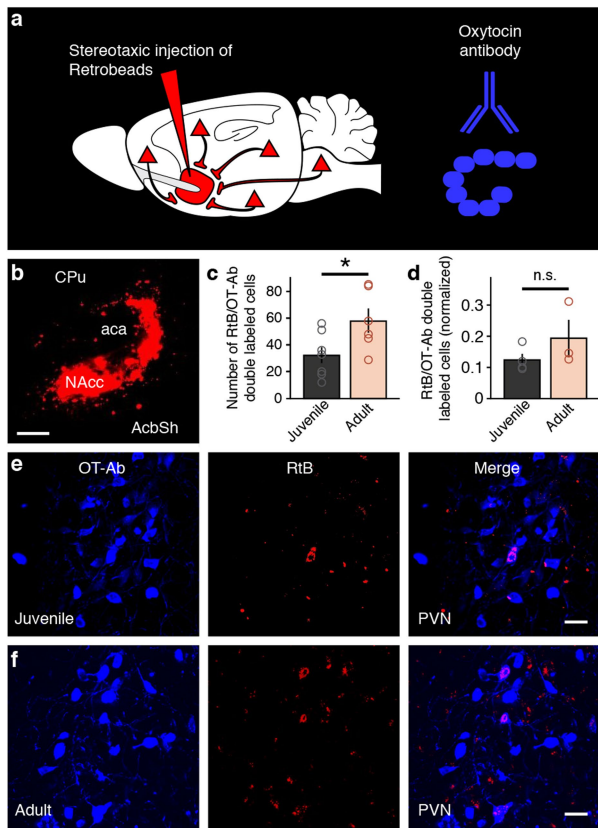
Extended Data Fig. 3 | The number of OT neurons projecting to the NAc does not decline during development. a, Injection and labelling strategy in C57BL/6 wild-type mice. **b**, Image showing successful targeting of NAc with retrobeads (RtBs). Scale bar, 500 μm. **c**, Quantification of RtB–OT antibody double-labelled cells across ages in the PVN (juvenile $n = 7$ animals; adult $n = 6$ animals; $t_{(11)} = -2.378$, $P = 0.037$; two-tailed unpaired t-test). **d**, Number of OT neurons innervating the NAc normalized to the total number of PVN neurons innervating the NAc shows that the developmental increase across ages is not restricted to OT projecting neurons (juvenile $n = 4$ animals; adult $n = 3$ animals; $t_{(5)} = -1.284$, $P = 0.256$; two tailed unpaired t-test). **e, f**, Images of the PVN labelled with OT antibodies (left) or RtB (centre) and merged (right) showing the presence of RtBs in OT neurons in both juvenile (**e**) and adult (**f**) mice. Scale bar, 50 μm. aca, anterior commissure; AcbSh, nucleus accumbens shell; CPu, caudate putamen; NAcc, nucleus accumbens core; PVN, paraventricular nucleus of the hypothalamus. Data are presented as mean ± s.e.m. *$P < 0.05$.
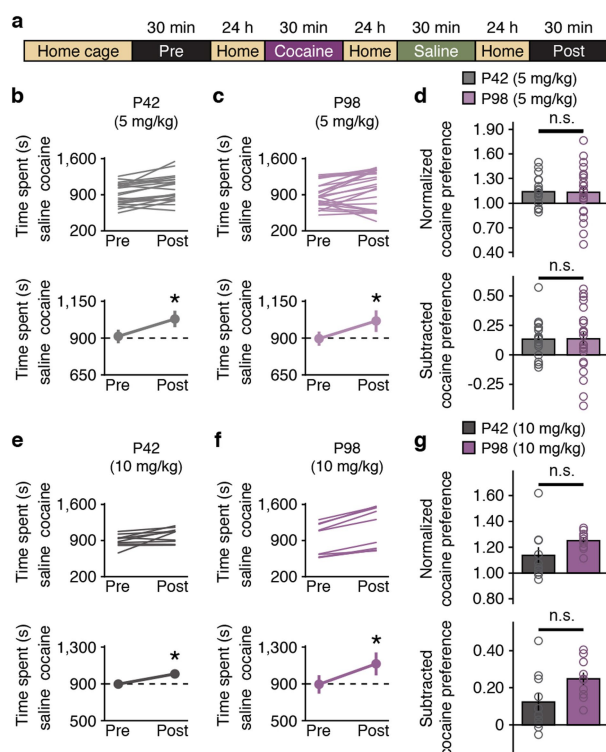
Extended Data Fig. 4 | Cocaine CPP (cCPP) is not different across the ages at lower doses of cocaine. a, Experimental time course of i.p. injections during cCPP experiments in **b**–**g**. **b**, **c**, Individual (top) and average (bottom) time spent in the cocaine-paired context indicates a significantly increased preference for the cocaine context after conditioning with 5 mg kg^{-1} cocaine (P42, $n = 20$ animals, $t_{(19)} = -3.701$, $P = 0.002$; P98, $n = 24$ animals, $t_{(23)} = -2.496$, $P = 0.020$; two-tailed paired t-test). **d**, Comparisons between P42 and P98 reveal no difference in normalized cocaine preference (top, $t_{(42)} = -0.029$, $P = 0.977$) and subtracted cocaine preference (bottom, $t_{(42)} = 0.121$, $P = 0.904$) with 5 mg kg^{-1} cocaine (two-tailed unpaired t-test). **e**, **f**, Individual (top) and average (bottom) time spent in the cocaine-paired context indicates a significantly increased preference for the cocaine context after conditioning with 10 mg kg^{-1} cocaine (P42, $n = 10$ animals, $t_{(9)} = -2.469$, $P = 0.036$; P98, $n = 10$ animals, $t_{(9)} = -7.411$, $P < 0.0001$; two-tailed paired t-test). **g**, Comparisons between P42 and P98 reveal no difference in normalized cocaine preference (top, $t_{(18)} = -1.698$, $P = 0.107$) and subtracted cocaine preference (bottom, $t_{(18)} = -2.07$, $P = 0.053$) with 10 mg kg^{-1} cocaine (two-tailed unpaired t-test). Data are presented as mean $\pm$ s.e.m. *$P < 0.05$; n.s., comparisons not significant ($P > 0.05$).
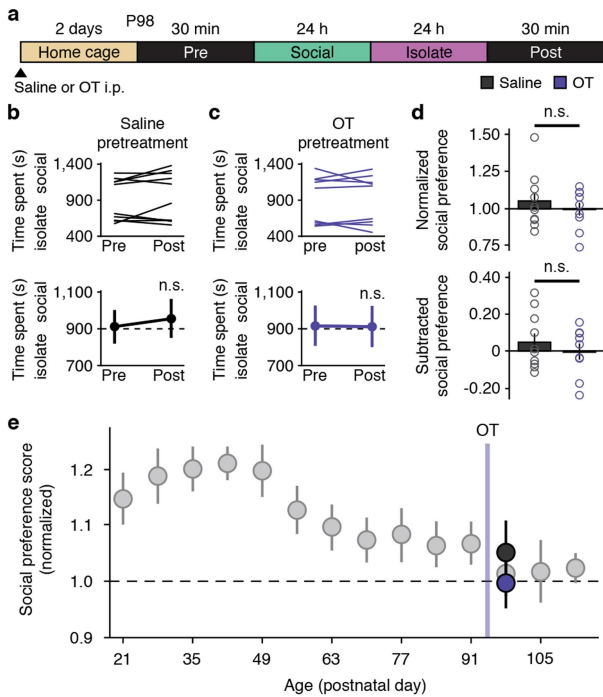
Extended Data Fig. 5 | Intraperitoneal OT does not reopen the critical period for social reward learning. a–e, Social CPP in adult animals following pretreatment with i.p. OT (0.5 mg kg^{-1}) or saline.
a, Experimental time course. **b, c**, Individual (top) and average (bottom) preference for the social context in animals receiving i.p. pretreatment with saline (**b**, $n = 10$ animals, $t_{(9)} = -1.049$, $P = 0.321$) or OT (**c**, $n = 9$ animals, $t_{(8)} = 0.126$, $P = 0.903$) (two-tailed paired t-test). **d**, Comparisons of the normalized (top, $t_{(17)} = 0.706$, $P = 0.49$) and subtracted (bottom, $t_{(17)} = 0.852$, $P = 0.406$) social preference reveal no difference between i.p. OT and saline pretreatment groups (two-tailed unpaired t-test).
e, Normalized social preference in mice pretreated with i.p. OT or saline plotted against the developmental time course of normalized social preference scores of untreated male mice (replotted from Fig. 1q). Data are presented as mean ± s.e.m. *$P < 0.05$; n.s., comparisons not significant ($P > 0.05$).
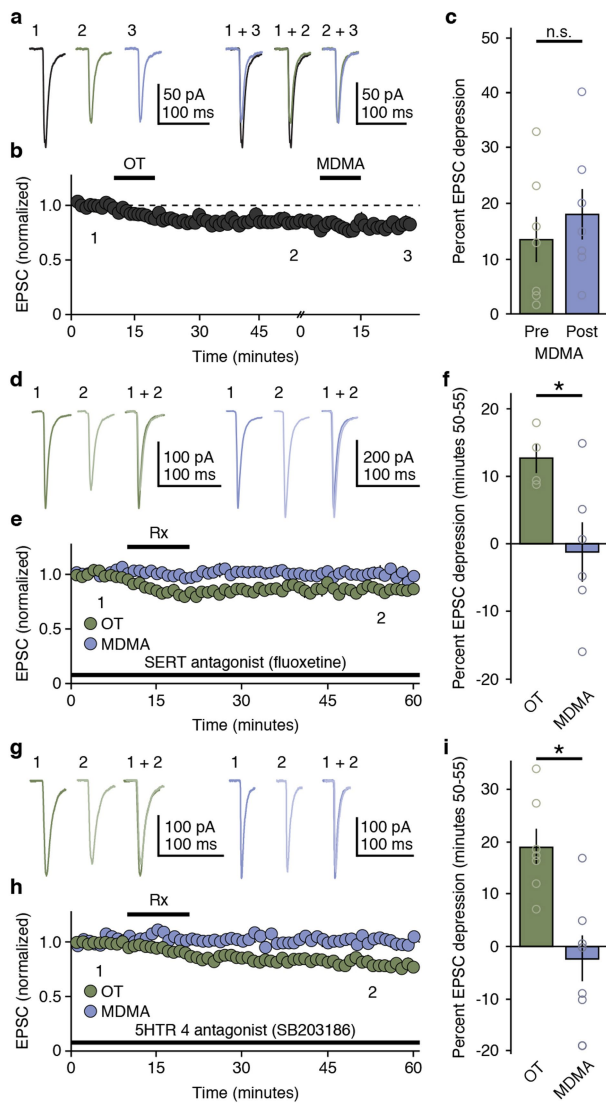
Extended Data Fig. 6 | MDMA-induced LTD in the NAc requires OTR, SERT, and 5HTR4 activation. a–i, Representative traces (**a, d, g**), summary time course (**b, e, h**), and average post-treatment magnitude comparisons (**c, f, i**) reveal that OT-LTD occludes MDMA-induced LTD (**a–c**, $n = 7$ cells, $t_{(6)} = 1.639$, $P = 0.152$; two-tailed paired t-test). The SERT antagonist fluoxetine (10 μM) blocks MDMA-induced but not OT-induced LTD (**d–f**, MDMA ($n = 6$ cells), OT ($n = 4$ cells), $t_{(8)} = 2.429$, $P = 0.041$; two-tailed unpaired t-test). The 5HTR4 antagonist SB203186 (10 μM) blocks MDMA-LTD but not OT-LTD (**g–i**, $n = 7$ cells, $t_{(12)} = 3.818$, $P = 0.002$; two tailed unpaired t-test). *$P < 0.05$; n.s., comparisons not significant ($P > 0.05$).
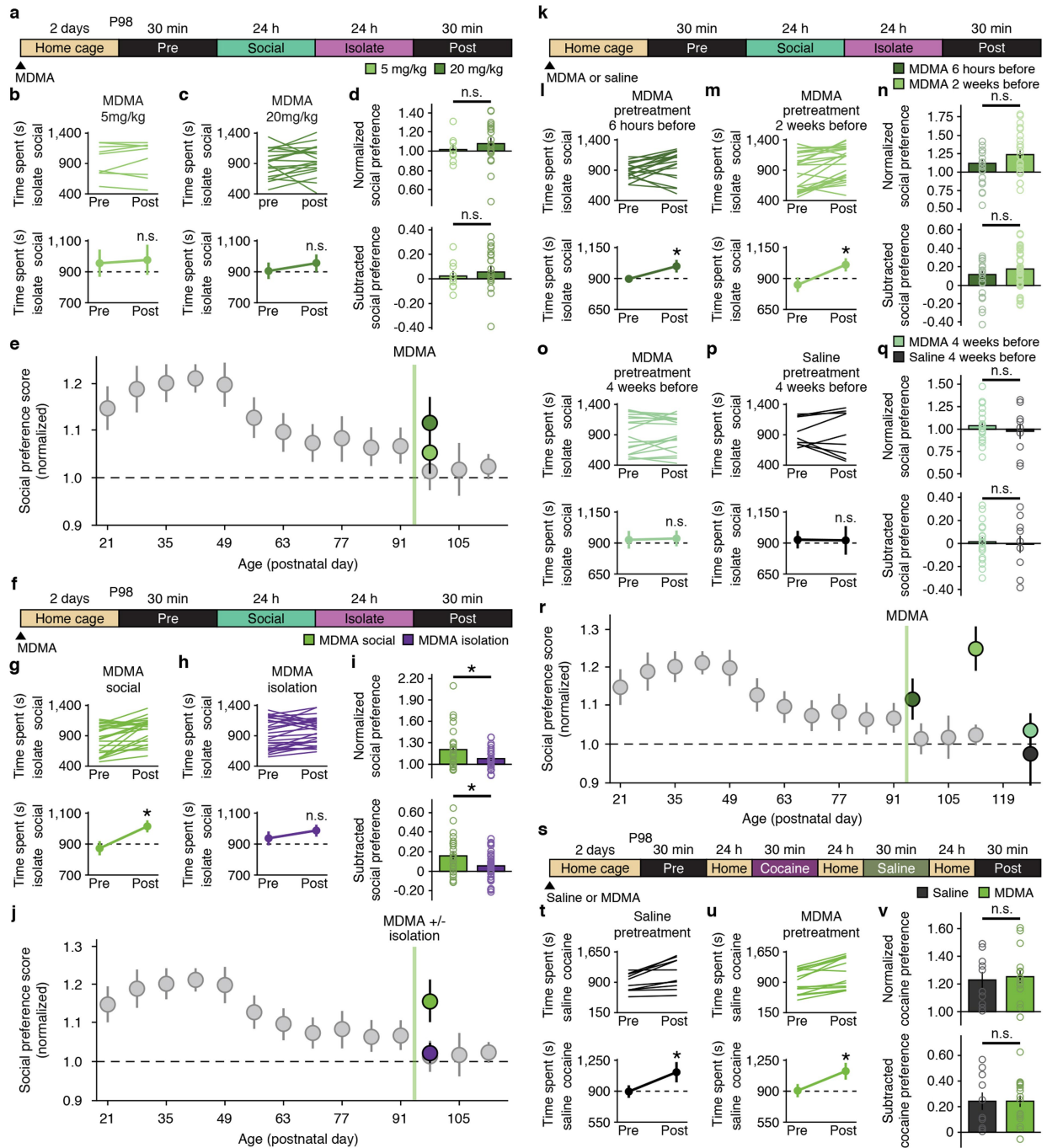
Extended Data Fig. 7 | See next page for caption.

Extended Data Fig. 7 | Dose, time course and social context of MDMA-induced reinstatement of social CPP in adult mice.
a, f, k, Experimental time course of i.p. pretreatment in social CPP.
a–e, Social CPP following pretreatment with i.p. MDMA at 5 mg kg^{-1} or 20 mg kg^{-1} shows that neither 5 mg kg^{-1} (**b**, $n = 9$ animals, $t_{(8)} = -0.61$, $P = 0.559$) nor 20 mg kg^{-1} (**c**, $n = 19$ animals, $t_{(18)} = -1.071$, $P = 0.298$) reopens the critical period for social reward learning (individual data, top; group average, bottom; two-tailed unpaired t-test). Comparisons of the normalized (top) and subtracted (bottom) social preference scores reveal no difference between 5 mg kg^{-1} and 20 mg kg^{-1} MDMA pretreatment groups (**d**, normalized, $t_{(26)} = -0.736$, $P = 0.468$; subtracted, $t_{(26)} = -0.384$, $P = 0.704$; two-tailed paired t-test). **e,** Normalized social preference in groups pretreated with MDMA (5 mg kg^{-1} or 20 mg kg^{-1}) plotted against the developmental time course of normalized social preference scores of untreated male mice (replotted from Fig. 1q).
**f–j,** i.p. MDMA injection followed by 3 h in social or isolate context shows that MDMA pretreatment reinstates social CPP when given in a social (**g**, $n = 26$ animals, $t_{(25)} = -4.116$, $P < 0.0004$) but not isolate (**h**, $n = 29$ animals, $t_{(28)} = -1.97$, $P = 0.059$) context. The social preference score following MDMA + 3 h isolation is lower than that following MDMA + 3 h social (**i**, normalized, $t_{(53)} = 2.239$, $P = 0.029$; subtracted, $t_{(53)} = 2.185$, $P = 0.033$; two-tailed unpaired t-test). **j,** Normalized social preference in groups pretreated with MDMA followed by 3 h isolation or 3 h social setting plotted against the developmental time course of normalized social preference scores of untreated male mice (replotted from Fig. 1q).

k–r, Following pretreatment with i.p. MDMA, reinstatement of social CPP is apparent after 6 h (**l**, $n = 19$, $t_{(18)} = -2.266$, $P = 0.036$), lasts at least 2 weeks (**m**, $n = 25$, $t_{(24)} = -4.421$, $P < 0.0001$) and returns to saline-pretreated levels by 4 weeks following MDMA pretreatment (**o**, MDMA, $n = 19$, $t_{(18)} = -0.319$, $P = 0.753$; **p**, saline $n = 9$, $t_{(8)} = 0.098$, $P = 0.924$) (two-tailed paired t-test). There is no difference between the 6-h and 2-week MDMA pretreatment groups (**n**, normalized ($t_{(42)} = -1.611$, $P = 0.115$; subtracted, $t_{(42)} = -1.011$, $P = 0.318$) or the MDMA and saline pretreatment groups 4 weeks after treatment (**q**, normalized, $t_{(26)} = 0.701$, $P = 0.49$; subtracted, $t_{(26)} = 0.258$, $P = 0.799$) (two-tailed unpaired t-test).
r, Normalized social preference in groups pretreated with MDMA (6 h, 2 and 4 weeks) and saline (4 weeks) plotted against the developmental time course of normalized social preference scores of untreated male mice (replotted from Fig. 1q). **s–v,** cCPP following pretreatment with i.p. MDMA. **s,** Experimental time course of i.p. injections before and during cCPP experiments in **t–v**. **t, u,** Individual (top) and average (bottom) time spent in the cocaine-paired context indicates a significantly increased preference for the cocaine (20 mg kg^{-1}) context after conditioning (saline, $n = 10$ animals, $t_{(9)} = -3.562$, $P = 0.006$; MDMA, $n = 16$ animals, $t_{(15)} = -5.477$, $P < 0.0001$, two-tailed paired t-test). **v,** Comparisons between mice pretreated with saline and MDMA 2 days before cCPP reveals no difference in normalized cocaine preference ($t_{(24)} = -0.322$, $P = 0.75$) or subtracted cocaine preference ($t_{(24)} = -0.001$, $P = 0.999$) (two-tailed unpaired t-test). Data are presented as mean $\pm$ s.e.m. *$P < 0.05$; n.s., comparisons not significant ($P > 0.05$).
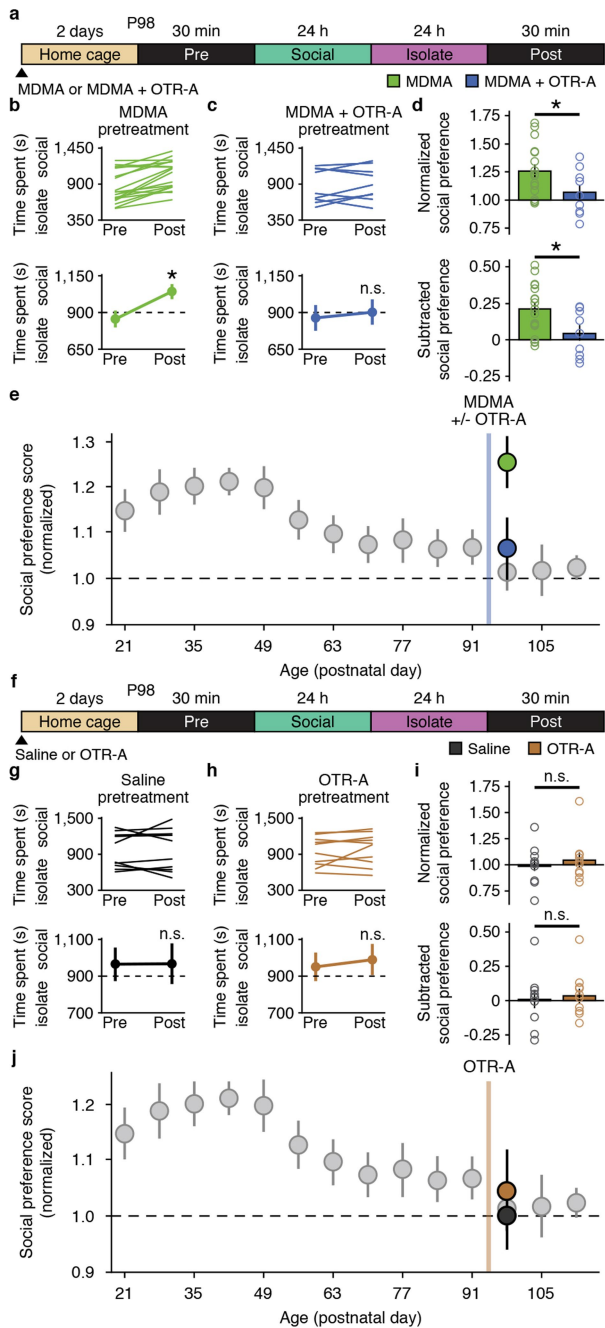
Extended Data Fig. 8 | OT receptor antagonist prevents the reopening of the critical period for social reward learning by MDMA. a–e, Social CPP in adult mice following pretreatment with i.p. MDMA or MDMA + OTR-A. **f–j,** Social CPP in adult mice following pretreatment with OTR-A or saline. **a, f,** Experimental time course of intraperitoneal (i.p.) pretreatment in social CPP. **b, c, g, h,** Individual (top) and average (bottom) responses to social CPP in mice pretreated with i.p. MDMA (**b**), MDMA + OTR-A (**c**), saline (**g**) or OTR-A (**h**). **b,** The reopening of the critical period for social reward learning by MDMA ($n = 18$ animals, $t_{(17)} = -5.182$, $P < 0.0001$) is abolished in the presence of OTR-A (**c,** $n = 9$ animals, $t_{(8)} = -0.837$, $P = 0.427$) (two-tailed paired t-test). **g, h,** There is no difference in time spent in social bedding cue following conditioning between animals pretreated with i.p. saline (**g,** $n = 10$ animals, $t_{(9)} = -0.057$, $P = 0.956$) or OTR-A ($n = 10$ animals, $t_{(9)} = -0.81$, $P = 0.439$) (two-tailed paired t-test). **d, i,** Comparisons of the normalized (top) and subtracted (bottom) social preference scores between treatment groups reveal a decrease following MDMA + OTR-A versus MDMA alone (**d,** normalized, $t_{(25)} = 2.106$, $P = 0.045$; subtracted, $t_{(25)} = 2.410$, $P = 0.024$) but no difference in OTR-A versus saline (**i,** normalized, $t_{(18)} = -0.587$, $P = 0.564$; subtracted, $t_{(18)} = -0.479$, $P = 0.638$) (two-tailed unpaired t-test). **e, j,** Normalized social preference in mice pretreated with MDMA or MDMA + OTR-A (**e**) and OTR-A or saline (**j**) plotted against the developmental time course of normalized social preference scores of untreated male mice (re-plotted from Fig. 1q). Data are presented as mean ± s.e.m. *$P < 0.05$; n.s., comparisons not significant ($P > 0.05$).
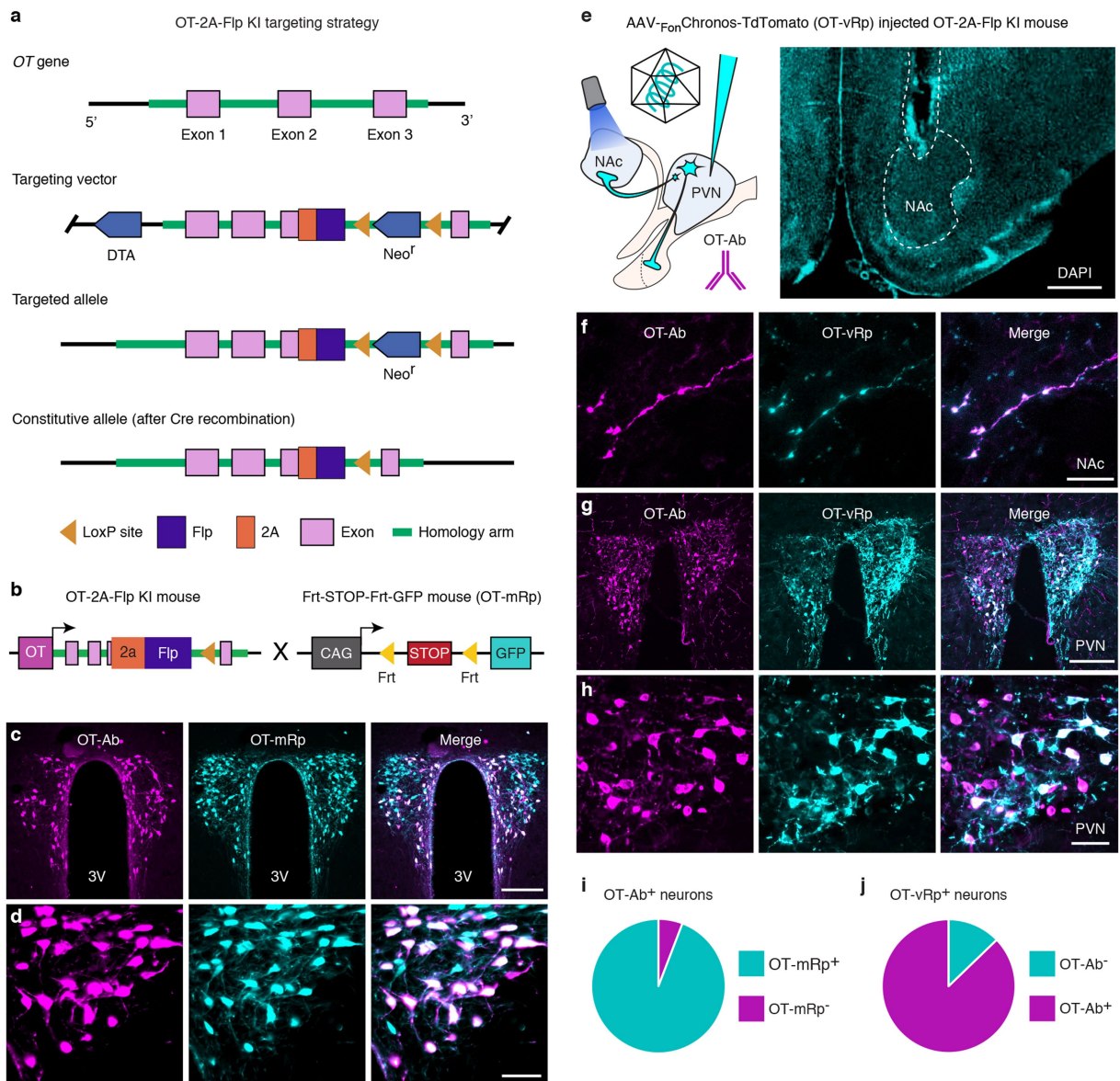
Extended Data Fig. 9 | Generation and validation of OT-2A-Flp knock-in mice and validation of optogenetic targeting strategy. a, Targeting strategy for generating an OT-2A-Flp knock-in (KI) mouse. **b–d, i**, The OT-2A-Flp::FonGFP cross efficiently labels OT neurons in the PVN of adult male mice. **b**, Breeding strategy for OT-2A-Flp driver mice crossed to FonGFP reporter mice. **c, d**, Representative image of the PVN labelled with OT antibody (OT-Ab, magenta, left), OT-2A-Flp::FonGFP (OT-mRP, cyan, centre), and merged (right) at low magnification (scale bar, 200 μm) and high magnification (scale bar, 50 μm). GFP expression (OT-mRp) under the OT promoter is co-localized with OT-Ab labelling in the PVN. **i**, In the PVN, OT-mRp is expressed in 94% of OT-Ab-labelled neurons ($n = 2$ animals; 714 ± 142 OT neurons per animal). **e–h, j**, Confirmation of viral expression, OT neuronal specificity, and probe placement in AAV-CAG-FonChronos-TdTomato (OT-vRp)/OT-2A-Flp KI mouse. **e**, Anatomical validation of optogenetic targeting strategy. Left, cell type specification and projection targeting strategy (adapted from ref. [40] with permission: https://creativecommons.org/licenses/by-nc-nd/4.0/). Right, DAPI staining to confirm optical probe placement above the NAc (scale bar, 1 mm). **f**, OT-Ab labelling (magenta, left) and Chronos-TdTomato expression (OT-vRp, cyan, middle) are co-localized (right) in axons in the NAc. **g, h**, OT-Ab labelling (magenta, left) and Chronos-TdTomato expression (OT-vRp, cyan, middle) are co-localized (right) in the PVN at low magnification (**c**, scale bar, 200 μm) and high magnification (**d**, scale bar, 50 μm). **j**, In the PVN, 87% of OT-vRp positive neurons are labelled by OT-Ab ($n = 3$ animals; 492 ± 112 OT neurons per animal). 3V, third ventricle.
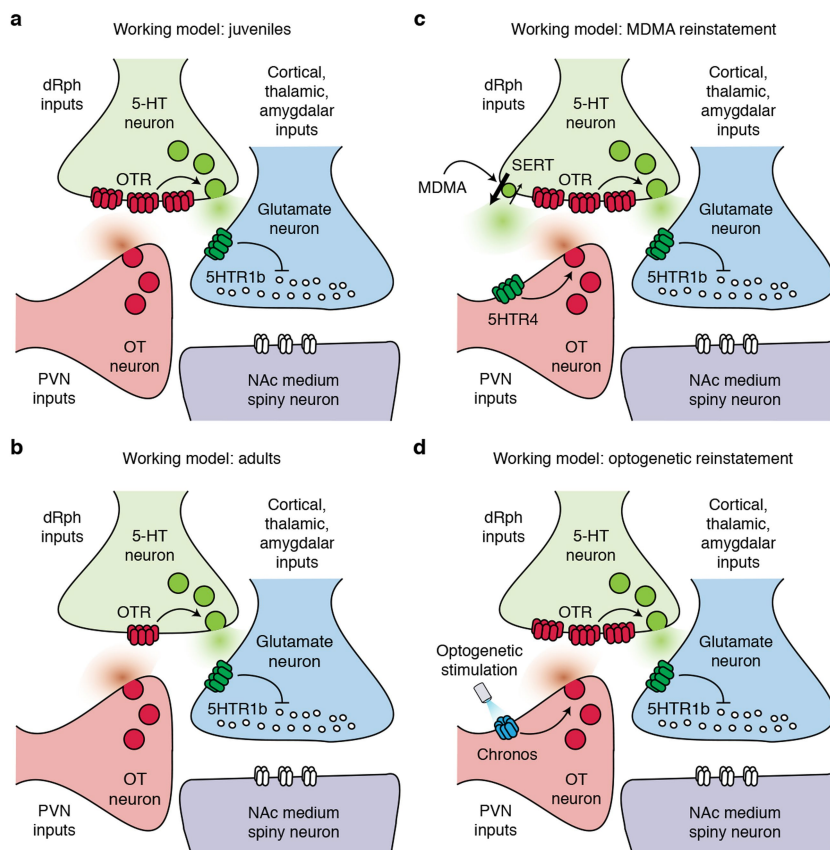
Extended Data Fig. 10 | Working model. a, In juvenile animals, OT-producing neurons from the PVN release OT into the NAc. Activation of OTRs on presynaptic terminals of 5-HT neurons from the dorsal raphe nucleus (dRph) causes the release of 5-HT into the NAc. Activation of 5HT1b receptors on glutamatergic terminals from various brain regions (cortex, amygdala, thalamus) decreases the probability of glutamate release, which is recorded in MSNs as LTD of excitatory synaptic transmission. **b**, In adult mice, OTRs are downregulated in the NAc, decreasing the magnitude of social CPP and OT-LTD induced at excitatory synapses onto MSNs. **c**, Binding of MDMA to the SERT transporter causes efflux of 5-HT, which activates 5HT4 receptors on OT terminals, causing the release of OT. In turn, increased synaptic OT induces metaplastic upregulation of OTRs, reinstating social CPP and induction of OT-LTD at excitatory synapses. **d**, Optogenetic stimulation of OT terminals causes direct release of OT in the NAc, inducing metaplastic upregulation of OTRs and recapitulating the effects of MDMA.
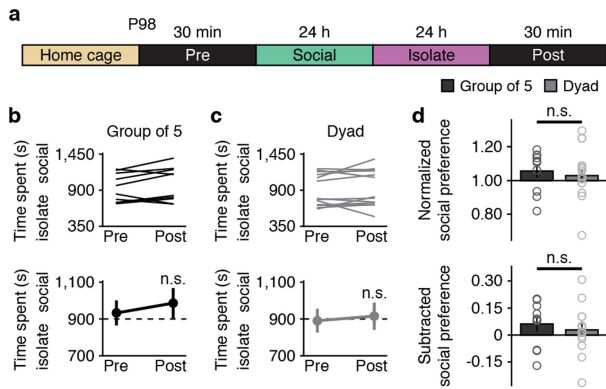
Extended Data Fig. 11 | Pair housing does not alter social reward learning in adults. a, Experimental time course for mice socially housed in groups of five versus pair housed (dyads) before social CPP. **b, c**, Individual (top) and average (bottom) responses in groups of five mice (**b**) versus dyads (**c**). Mice housed in groups of five or two show similar social preferences at P98 (group of five, $n = 10$ animals, $t_{(9)} = -1.472$, $P = 0.175$; dyad, $n = 14$ animals, $t_{(13)} = -0.742$, $P = 0.471$; two-tailed paired t-test). **d**, Comparisons between housing groups reveal no difference in normalized (top, $t_{(22)} = 0.502$, $P = 0.62$) or subtracted (bottom, $t_{(22)} = 0.595$, $P = 0.558$) social preference scores (two-tailed unpaired t-test). Data are presented as mean ± s.e.m. *$P < 0.05$; n.s., comparisons not significant ($P > 0.05$).

Extended Data Table 1 | Social reward learning across development in male mice

Age	Mean pre	Mean post	Paired t-test	Unpaired t-test Pre vs P42	Unpaired t-test Post vs P42	Mean normalized	Unpaired t-test normalized vs P42	Unpaired t-test normalized vs P98	Mean subtracted	Unpaired t-test subtracted vs P42	Unpaired t-test subtracted vs P98	n
P21	891 ± 38	1,002 ± 34	**0.007***	0.6822	0.3612	1.15 ± 0.05	0.2324	0.0364	0.12 ± 0.04	0.1362	0.0557	19
P28	897 ± 45	1,033 ± 29	**0.0005***	0.6198	0.8007	1.19 ± 0.05	0.669	0.0089	0.15 ± 0.04	0.3419	0.0178	20
P35	882 ± 31	1,038 ± 29	**<0.0001***	0.8046	0.8868	1.20 ± 0.04	0.827	**0.0019***	0.17 ± 0.03	0.6613	**0.0031***	30
P42	872 ± 29	1,043 ± 29	**<0.0001***	-	-	1.21 ± 0.03	-	**0.0003***	0.19 ± 0.02	-	**0.0005***	29
P49	887 ± 34	1,047 ± 41	**0.0001***	0.7219	0.9452	1.20 ± 0.05	0.7965	0.0054	0.18 ± 0.04	0.7613	0.0040	30
P56	905 ± 65	988 ± 57	**0.0093***	0.6062	0.3453	1.13 ± 0.04	0.1123	0.0660	0.09 ± 0.03	0.018	0.1139	19
P63	878 ± 65	937 ± 55	0.0949	0.9176	0.0672	1.10 ± 0.04	0.0302	0.1749	0.07 ± 0.04	0.0051	0.2567	18
P70	911 ± 45	970 ± 52	0.0849	0.4431	0.2025	1.07 ± 0.04	0.0075	0.3105	0.07 ± 0.04	0.0047	0.2233	23
P77	879 ± 56	959 ± 83	0.1000	0.8984	0.2427	1.08 ± 0.05	0.0264	0.3039	0.09 ± 0.05	0.0476	0.2014	14
P84	873 ± 40	931 ± 55	0.0747	0.9733	0.0734	1.07 ± 0.04	0.0057	0.3790	0.06 ± 0.03	0.004	0.2046	29
P91	868 ± 51	912 ± 55	0.1768	0.9446	0.0337	1.07 ± 0.04	0.0053	0.3407	0.05 ± 0.04	**0.0018***	0.3096	26
P98	958 ± 47	960 ± 56	0.9557	0.1137	0.1734	1.02 ± 0.04	**0.0003***	-	-0.02 ± 0.05	**0.0005***	-	25
P105	931 ± 40	945 ± 60	0.7797	0.2231	0.1126	1.02 ± 0.06	**0.0019***	0.9646	0.02 ± 0.05	**0.002***	0.6901	20
P112	895 ± 57	914 ± 60	0.3796	0.7015	0.0442	1.02 ± 0.03	**<0.0001***	0.8665	0.02 ± 0.02	**<0.0001***	0.5464	23

Pre, post, normalized and subtracted mean values for each age shown in Fig. 1. The data are presented as mean ± s.e.m. Two tailed paired t-test pre versus post, $*P < 0.05$. For unpaired t-test Bonferroni correction value for statistical significance, $*P < 0.0036$. n, number of animals.

naturesearch

Reporting Summary

Nature Research wishes to improve the reproducibility of the work that we publish. This form provides structure for consistency and transparency in reporting. For further information on Nature Research policies, see <u>Authors & Referees</u> and the <u>Editorial Policy Checklist</u>.

Statistics

For all statistical analyses, confirm that the following items are present in the figure legend, table legend, main text, or Methods section.

n/a	Confirmed	
☐	☒	The exact sample size (*n*) for each experimental group/condition, given as a discrete number and unit of measurement
☐	☒	A statement on whether measurements were taken from distinct samples or whether the same sample was measured repeatedly
☐	☒	The statistical test(s) used AND whether they are one- or two-sided *Only common tests should be described solely by name; describe more complex techniques in the Methods section.*
☐	☒	A description of all covariates tested
☐	☒	A description of any assumptions or corrections, such as tests of normality and adjustment for multiple comparisons
☐	☒	A full description of the statistical parameters including central tendency (e.g. means) or other basic estimates (e.g. regression coefficient) AND variation (e.g. standard deviation) or associated estimates of uncertainty (e.g. confidence intervals)
☐	☒	For null hypothesis testing, the test statistic (e.g. *F*, *t*, *r*) with confidence intervals, effect sizes, degrees of freedom and *P* value noted *Give P values as exact values whenever suitable.*
☒	☐	For Bayesian analysis, information on the choice of priors and Markov chain Monte Carlo settings
☐	☒	For hierarchical and complex designs, identification of the appropriate level for tests and full reporting of outcomes
☐	☒	Estimates of effect sizes (e.g. Cohen's *d*, Pearson's *r*), indicating how they were calculated

Our web collection on <u>statistics for biologists</u> contains articles on many of the points above.

Software and code

Policy information about <u>availability of computer code</u>

Data collection	For electrophysiology experiments, data acquisition was performed on-line using custom Igor Pro software. For behavioral experiments, the position of the mouse was monitored using a commercially available software interface (Activity Monitor, Med Associates).
Data analysis	For electrophysiology experiments, data analysis was performed on-line using custom Igor Pro software. For behavioral experiments, commercially available SPSS statistical program was used for analysis

For manuscripts utilizing custom algorithms or software that are central to the research but not yet described in published literature, software must be made available to editors/reviewers. We strongly encourage code deposition in a community repository (e.g. GitHub). See the Nature Research <u>guidelines for submitting code & software</u> for further information.

Data

Policy information about <u>availability of data</u>

All manuscripts must include a <u>data availability statement</u>. This statement should provide the following information, where applicable:

- Accession codes, unique identifiers, or web links for publicly available datasets
- A list of figures that have associated raw data
- A description of any restrictions on data availability

Figures 1, 2, 3 and 4 as well as Supplementary Figures 1,2,4,5,6,7,8,9,10,11,12,13,14,18,19,and 20 have associated raw data, which will be made available upon request.

Field-specific reporting

Please select the one below that is the best fit for your research. If you are not sure, read the appropriate sections before making your selection.

☒ Life sciences   ☐ Behavioural & social sciences   ☐ Ecological, evolutionary & environmental sciences

For a reference copy of the document with all sections, see nature.com/documents/nr-reporting-summary-flat.pdf

Life sciences study design

All studies must disclose on these points even when the disclosure is negative.

Sample size	Sample size was determined based on our previous findings and the published literature
Data exclusions	For behavioral studies, mice were excluded if they exhibited a pre-conditioning preference score > 1.5 or < 0.5. These criteria were established prior to testing.
Replication	In order to maximize data robustness, care was taken to use automated analysis protocols and validate all assays for inter-rater reliability.
Randomization	To assure unbiased design for behavioral experiments, chamber assignments were counterbalanced for side and place cues. Pharmacological delivery schedules were counterbalanced for type of drug (i.e. saline, MDMA, cocaine).
Blinding	For behavioral experiments, blinding for age was not possible, since the experimenters were intimately familiar with the appearance of animals at each age. For optogenetic and pharmacological manipulations, experimenter was blind to treatment condition during behavioral scoring, which was automated to ensure unbiased data analysis. Group allocations were randomized during data collection.

Reporting for specific materials, systems and methods

We require information from authors about some types of materials, experimental systems and methods used in many studies. Here, indicate whether each material, system or method listed is relevant to your study. If you are not sure if a list item applies to your research, read the appropriate section before selecting a response.

Materials & experimental systems

n/a	Involved in the study
☐	☒ Antibodies
☒	☐ Eukaryotic cell lines
☒	☐ Palaeontology
☐	☒ Animals and other organisms
☒	☐ Human research participants
☒	☐ Clinical data

Methods

n/a	Involved in the study
☒	☐ ChIP-seq
☒	☐ Flow cytometry
☒	☐ MRI-based neuroimaging

Antibodies

Antibodies used	Oxytocin-NP PS-38 antibody, gift of Harold Gainer;
Validation	Original Validation: Whitnall et al., Journal of Neuroscience 1985 5:1,98-109 and Ben-Barak et al., Journal of Neuroscience 1985 5:1,81-97.

Animals and other organisms

Policy information about studies involving animals; ARRIVE guidelines recommended for reporting animal research

Laboratory animals	C57BL/6 or OT-2A-FlpO mice on the C57BL/6 background were used for all experiments.
Wild animals	Study did not involve wild animals
Field-collected samples	Study did not involve field collected samples
Ethics oversight	All procedures complied with the animal care standards set forth by the National Institutes of Health and were approved by the host institution's Administrative Panel on Laboratory Animal Care.

Note that full information on the approval of the study protocol must also be provided in the manuscript.

nature research

Corresponding author(s):

Double-blind peer review submissions: write DBPR and your manuscript number here instead of author names.

Last updated by author(s): *YYYY-MM-DD*

Editorial Policy Checklist

This form is used to ensure compliance with Nature Research editorial policies related to research ethics and reproducibility. For further information, please see our Authors & Referees site. All relevant questions on the form must be answered.

Competing interests

Policy information about competing interests

Competing interests declaration

In the interest of transparency and to help readers form their own judgements of potential bias, Nature Research journals require authors to declare any competing financial and/or non-financial interest in relation to the work described in the submitted manuscript.

☒ We declare that none of the authors have competing financial or non-financial interests as defined by Nature Research.

☐ We declare that one or more of the authors have a competing interest as defined by Nature Research.

Authorship

Policy information about authorship

Prior to submission all listed authors must agree to all manuscript contents, the author list and its order and the author contribution statements. Any changes to the author list after submission must be approved by all authors.

☒ We have read the Nature Research Authorship Policy and confirm that this manuscript complies.

Data availability

Policy information about availability of data

Data availability statement

All manuscripts must include a data availability statement. This statement should provide the following information, where applicable:

- Accession codes, unique identifiers, or web links for publicly available datasets
- A list of figures that have associated raw data
- A description of any restrictions on data availability

☒ We have provided a full data availability statement in the manuscript.

Mandated accession codes (where applicable)

Confirm that all relevant data are deposited into a public repository and that accession codes are provided.

☒ All relevant accession codes are provided   ☐ Accession codes will be available before publication   ☐ No data with mandated deposition

Code availability

Policy information about availability of computer code

Code availability statement

For all studies using custom code or mathematical algorithm that is deemed central to the conclusions, the Methods section must include a statement under the heading "Code availability" describing how readers can access the code, including any access restrictions.

☒ We have provided a full code availability statement in the manuscript

Data presentation

For all data presented in a plot, chart or other visual representation confirm that:

n/a	Confirmed	
☐	☒	Individual data points are shown when possible, and always for $n \leq 10$
☐	☒	The format shows data distribution clearly (e.g. dot plots, box-and-whisker plots)
☐	☒	Box-plot elements are defined (e.g. center line, median; box limits, upper and lower quartiles; whiskers, 1.5x interquartile range; points, outliers)
☐	☒	Clearly defined error bars are present and what they represent (SD, SE, CI) is noted

Image integrity

Policy information about image integrity

☒ We have read Nature Research's image integrity policy and all images comply.

Unprocessed data must be provided upon request. Please double-check figure assembly to ensure that all panels are accurate (e.g. all labels are correct, no inadvertent duplications have occurred during preparation, etc.).

Additional policy considerations

Some types of research require additional policy disclosures. Please indicate whether each of these apply to your study. If you are not certain, please read the appropriate section before selecting a response.

Does not apply	Involved in the study
☒	☐ Macromolecular structural data
☐	☒ Unique biological materials
☐	☒ Research animals and/or animal-derived materials that require ethical approval
☒	☐ Human embryos, gametes and/or stem cells
☒	☐ Human research participants
☒	☐ Clinical data

Biological materials

Policy information about availability of materials

Obtaining biological materials — *Describe any restrictions on the availability of unique materials OR confirm that all unique materials used are readily available from the authors or from standard commercial sources (and specify these sources).*

☐ We have described these restrictions in the manuscript.   ☒ We have described how to obtain all materials in the manuscript.

Research animals

Policy information about studies involving animals; ARRIVE guidelines recommended for reporting animal research

Ethical compliance
☒ We have complied with all relevant ethical regulations and include a statement affirming this in the manuscript.

Ethics committee
☒ We have disclosed the name(s) of the board and institution that approved the study protocol in the manuscript.

I certify that all the above information is complete and correct.

Typed signature: DBPR   Date 1/8/2019